PSU/TURBO 82-4

SEMI-ANNUAL PROGRESS REPORT ON
THREE DIMENSIONAL FLOW FIELD INSIDE COMPRESSOR ROTOR, INCLUDING BLADE BOUNDARY LAYERS

J. M. GALMES, M. POUAGARE, AND B. LAKSHMINARAYANA

NASA GRANT NSG 3266

NATIONAL AERONAUTICS & SPACE ADMINISTRATION

LEWIS RESEARCH CENTER

TURBOMACHINERY LABORATORY
DEPARTMENT OF AEROSPACE ENGINEERING
THE PENNSYLVANIA STATE UNIVERSITY
UNIVERSITY PARK, PA 16802

JUNE 1982

PSU-Turbo-82-4

Semi-Annual Progress Report

on

THREE DIMENSIONAL FLOW FIELD INSIDE COMPRESSOR ROTOR PASSAGES, INCLUDING BLADE BOUNDARY LAYERS

J. M. Galmes, M. Pouagare, and B. Lakshminarayana

to

NASA Lewis Research Center

Project Monitor: Dr. P. Sockol

Turbomachinery Laboratory

Department of Aerospace Engineering

The Pennsylvania State University

University Park, PA 16802

June 1982

PREFACE

The progress of research on "Three Dimensional Flow Field Inside a Compressor Rotor Blade Passage, Including Blade Boundary Layers" (NASA Grant NSG 3266) for the six-month period ending June 30, 1982, is briefly reported here. Two papers were presented and published during this period. These are listed in section 5 of the report.

B. Lakshminarayana
Principal Investigator

TABLE OF CONTENTS

NOMENCLATURE

a^r_{mik}	fourth order tensor in pressure strain correlation model
b_{ij}	$\frac{\overline{u_i u_j}}{2k} - \frac{1}{3}\delta_{ij}$
c	chord length
C_p, C_1, C_μ $C_{\varepsilon_1}, C_{\varepsilon_2}, C_{\varepsilon_3}$	modeling constants
$F_\varepsilon(R_T, R_{ic})$	dumping function for low Reynolds number flows
g_{ik}	metric tensor
$k = \frac{1}{2} g^{ik} \overline{u_i' u_k'}$	turbulent kinetic energy
ℓ	length scale
N	distance normal to blade, normalized by blade spacing
p, p'	pressure, fluctuating pressure
$\bar{P}$	mean pressure
P, P_{ik}	turbulence production
r	radial distance to the axis in equation 39
q	vector of unknowns
R	radial distance normalized by the tip radius
$R_T = \frac{k^2}{\nu\varepsilon}$	local Reynolds numbers
$R_{ic} = -\frac{\varepsilon_{ipj}\Omega^p}{\bar{U}_{i,j}}$	generalized gradient Richardson number
S_{ij}	strain tensor
T	shear stress
u', u'^i	fluctuating velocity
$\bar{U}^i$	mean contravariant velocity
$U^{*m}_{,\ell} = \bar{U}^m_{,\ell} + \varepsilon^m_{p\ell}\,\Omega^p$	

$\overline{u_i' u_j'}$	Reynolds tensor
U_e	local freestream (or edge) velocity
U_s	streamwise relative velocity normalized by U_e
W,V,U	velocities in radial, tangential, and axial direction, respectively
x^j, x_j	contravariant and covariant coordinates variables
z,n,r	streamwise, normal, and radial directions (orthogonal to each other shown in Fig. 12, z = 0 at leading edge, n = 0 on the blade, r = 0 at the machine axis)
x,y	distance along and normal to cylinder (Figs. 2-12)
Z	chordwise distance normalized by the blade chord
δ	boundary layer thickness
δ_{ij}	Kronecker tensor
$\varepsilon = 2\nu \overline{s_{ij}' s'^{ij}}$	turbulent dissipation rate
ε_{ipj}	permutation tensor
μ	molecular viscosity
μ_{eff}	$\mu + \mu_T$
μ_T	turbulent viscosity
τ_z	$\sqrt{\overline{U'^2}}/U_e$
τ_r	$\sqrt{\overline{W'^2}}/U_e$
ρ	density
$\sigma_k, \sigma_\varepsilon, \sigma_w$	modeling constants
Ω	angular velocity
Ω^p	contravariant component of angular velocity

Subscripts

i,j,k,ℓ,m,n	indices
e	edge

1. TURBULENCE MODELLING: REYNOLDS STRESS MODEL (RSM)

A literature survey on both the analytical and the experimental work on effects of curvature and/or rotation was given in ref. 1. Some of the important conclusions of that survey were:

1. Only few calculations are available for the prediction of the three dimensional boundary layer in rotating frames.

2. No complete Reynolds stress model is available for rotating turbulent flows. Very few attempts have been made to account for the rotation effects in the k-ε model and those are not based on a logical analysis.

3. There are very few detailed measurements providing information on the effects of both the Rossby and the Richardson number on turbulence.

It was emphasized in ref. 1 that new experimental results would be of great interest, particularly if the rotation effect can be isolated from the other effects. It was also noted that a major effort should be given to the analysis of the dissipation rate equation and to the Reynolds stress equations.

In the previous report [1], modelling of the rotation effect and the low Reynolds number effect in the dissipation and the kinetic energy equations were described, with major emphasis on the equation for the dissipation rate. It was also noticed that, in the case of a k-ε model, the assumption of the existence of an eddy viscosity concept could not account for the anisotropy of the turbulence which exists in the boundary layer around a blade. The best way to avoid this problem would be to solve the complete set of Reynolds stresses equations along with the momentum equations.

However, the calculation procedures for three-dimensional viscous flows require large memory storage and large computer CPU time to solve the three momentum and continuity equations. The resolution of the six Reynolds stress

equations simultaneously with the three momentum equations, the continuity equation, and an equation for the dissipation rate is a very complex problem and can still be considered as an unresolved one. It is hoped that the rapid progress in computers and also the progress made in developing calculation algorithms for three-dimensional viscous flows will allow such calculations to be done in the very near future.

A two-equation model is a compromise between a full Reynolds stress model and the empirical models which fail to represent the turbulence properties in such complex flows as rotor blade boundary layer. However, the anisotropy of turbulence which exists in flows cannot be represented by the usual isotropic eddy viscosity formulation. In its more general form, the eddy viscosity is a fourth order tensor which depends on many parameters such as the Reynolds tensor, the strain tensor, the curvature and the rotation. It is therefore, a very complex formulation, which evidently represents very complex phenomenon. At this stage of the discussion it appears that the eddy viscosity tensor could be as difficult to handle as a Reynolds stress model. For the cases which are of interest to us, e.g. blade boundary layers, an algebraic model of the Reynolds stresses based on the complete model, together with the dissipation equation might be a compromise between a detailed description of the turbulent stresses (full Reynolds stress model) and the very crude eddy viscosity hypothesis.

It is not necessary to solve the complete set of equations for the Reynolds stresses, it is, however, necessary to analyze the Reynolds stress equation to find out which terms have to be modelled or neglected and then derive some propositions to model the remaining terms.

1.1 Reynolds Stress Equation

The equations of the mean and turbulent quantities for an incompressible flow in the generalized tensor formulation are given in ref. 1. The Reynolds stress equation which is of interest in the discussion that follows is given by:

$$(\rho\overline{u'_i u'_k})+(\rho\overline{u'_i u'_k}\,\bar{U}^j)_{,j} = -(\overline{p'u'_i}\delta^j_k + \overline{p'u'_k}\,\delta^j_i + \rho\,\overline{u'_i u'_k u'^j} - \overline{u'_i F^j_k} - \overline{u'_k F^j_i})_{,j}$$

$$+ \overline{p'u'_{i,j}}\,\delta^j_k + \overline{p'u'_{k,j}}\,\delta^j_i - \rho\overline{u'_i u'^j}(\bar{U}_{k,j} + 2\Omega^P\varepsilon_{kpj}) - \rho\overline{u'_k u'^j}(\bar{U}_{i,j} + 2\Omega^P\varepsilon_{ipj})$$

$$- \overline{F^j_k u'_{i,j}} - \overline{F^j_i u'_{k,j}} \qquad F_{ik} = 2\mu\, S_{ik} \qquad (1)$$

It is evident that the Reynolds stresses appear to be affected explicitly by the Coriolis forces, but they are also implicitly affected by the rotation through the triple velocity correlations, the pressure velocity correlations, the pressure strain correlation, the production by the stresses themselves, and the dissipation.

In the case of a Reynolds stress equation model, the second order terms are handled exactly, then only dissipation, pressure strain correlation and diffusion terms need to be analyzed and modelled.

These quantities must be represented as empirical functions of the mean velocities, Reynolds stresses, and their derivatives and the rotation and curvature. These terms will be analyzed and modelled separately.

1.2 Pressure-Strain Correlation

$$\overline{p'u'_{i,j}}\,\delta^j_k + \overline{p'u'_{kj,j}}\,\delta^j_i = \overline{p'u'_{i,k}} + \overline{p'u'_{k,i}}$$

Following Chou [2], the explicit appearance of the pressure may be eliminated by taking the divergence of the equation for fluctuating velocity u'_ℓ, thus obtaining a Poisson equation for the fluctuation p'.

The fluctuating Navier-Stokes equation is:

$$(\rho\dot{u}'_\ell)+(\rho\bar{U}_\ell u'^r+\rho u'_\ell\bar{U}^r+\rho u'_\ell u'^r-\overline{\rho u'_\ell u'^r})_{,r}+2\varepsilon_{\ell pr}\rho\Omega^p u'^r=-(p'\delta^r_\ell-F'^r_\ell)_{,r} \tag{3}$$

let us then take the divergence of equation 3

$$g^{\ell m}(\rho\dot{u}'_\ell)_{,m}+g^{\ell m}(\rho\bar{U}_\ell u'^r+\rho u'_\ell\bar{U}^r+\rho u'_\ell u'^r-\overline{\rho u'_\ell u'^r})_{,rm}+2g^{\ell m}(\varepsilon_{\ell pr}\rho\Omega^p u'^r)_{,m}=-g^{\ell m}(p'\delta^r_\ell-F'^r_\ell)_{,rm}$$

and with the continuity equation: $\bar{U}^i_{,i}=0\ ;\ u'^i_{,i}=0$

we may re-write this equation.

a) the time and space derivative are commutable, then the time derivative disappears

b) the viscous term also disappears.

$$\frac{\nabla^2 p'}{\rho}=(\overline{u'^m u'^r})_{,mr}-(u'^m u'^r)_{,mr}-2(\bar{U}^m_{,r}+\varepsilon^m_{pr}\Omega^p)u'^r_{,m} \tag{4}$$

which is the Poisson equation for the pressure fluctuation.

Then following Chou, the pressure fluctuation may be expressed in the following form for a position x in the flow.

$$\frac{p'(x)}{\rho}=\frac{1}{4\pi}\iiint_{vol}\{(u'^m_1u'^r_1)_{,mr_1}-(\overline{u'^m_1u'^r_1})_{,mr_1}\}\frac{dV'_1}{||\vec{\xi}||}$$

$$+\frac{1}{2\pi}\iiint_{vol}\{\bar{U}^m_{1,r_1}+\varepsilon^m_{pr}\Omega^p_1\}\,u'^r_{1,m_1}\frac{dV'_1}{||\vec{\xi}||}$$

$$+\frac{1}{4\pi\rho}\iint_S\{\frac{1}{||\vec{\xi}||}\frac{\partial p'_1}{\partial n_1}-p'_1\frac{\partial^1/||\vec{\xi}||}{\partial n_1}\}dS_1 \tag{5}$$

where terms with and without an indice 1 relate to values at x_1 and x, respectively (the integration being carried out over x_1 space) ($\vec{\xi}=\vec{x}_1-\vec{x}$).

An expression for the pressure strain correlation which appears in the equation of Reynolds stresses can be derived as follows. We calculate the correlation at point x, then $u'_{i,k}$ and $u'_{k,i}$ are independent of point x_1 and may be considered as constants for the volume and surface integrals.

Then we may write:

$$\frac{\overline{p'u'_{i,k}}}{\rho} = \phi_{ik,1} + \phi_{ik,2} + \zeta_{ik} = g_{i\ell}(\phi^{\ell}_{k,1} + \phi^{\ell}_{k,2} + \zeta^{\ell}_{k})$$

$$\frac{\overline{p'u'_{k,i}}}{\rho} = \phi_{ki,1} + \phi_{ki,2} + \zeta_{ki} = g_{k\ell}(\phi^{\ell}_{i,1} + \phi^{\ell}_{i,2} + \zeta^{\ell}_{i}) \qquad (6)$$

with:

$$\phi^{\ell}_{k,1} = \frac{1}{4\pi}\iiint_{vol} \overline{(u'^{m}_{1}u'^{r}_{1})_{,mr_1}\, u'^{\ell}_{,k}}\, \frac{dV'_1}{||\vec{\xi}||}$$

$$\phi^{\ell}_{k,2} = \frac{1}{2\pi}\iiint_{vol} \{\bar{U}^{m}_{1,r_1} + \varepsilon^{m}_{pr}\Omega^{p}_{1}\}\, \overline{u'^{r}_{1,m_1}u'^{\ell}_{i,k}}\, \frac{dV'_1}{||\vec{\xi}||}$$

$$\zeta^{\ell}_{k} = \frac{1}{4\pi\rho}\iint_{S} \{\frac{1}{||\vec{\xi}||}\overline{\frac{\partial p'_1}{\partial u_1}u'_{\ell,k}} - \overline{p'_1u'_{\ell,k}}\,\frac{\partial^1/||\vec{\xi}||}{\partial n_1}\} \qquad (7)$$

Equation 6 suggests that there are three distinct kinds of interaction giving rise to the pressure strain correlation; one involving fluctuating quantities $\phi^{\ell}_{k,1}$, another arising from the presence of "external effects" such as mean strain rate and rotation $\phi^{\ell}_{k,2}$; the last one is a surface integral which will be negligible away from the vicinity of a solid boundary [3].

Some of the proposals for closing the Reynolds stress equation have assumed that $\phi_{ik,1}$ is the only significant contribution to $\overline{pu_{i,k}}$ [4-6]. However, Reynolds [7] has shown that prediction of a range of even homogeneous

free turbulent flows demands the inclusion of mean strain rates in the pressure-strain terms. Moreover, both Townsend [8] and Crow [9] have shown that under conditions of rapid distortion the effect of $\phi_{ik,2}$ far outweighs that of $\phi_{ik,1}$.

It is then necessary to model $\phi_{ik,2}$ as well as $\phi_{ik.1}$.

1.2.1 Modelling of $\phi_{ik,2}$: "Rapid Term"

Our practice in simulating $\phi_{ik,2}$ and $\phi_{ki,2}$ takes its direction from Rotta's analysis and more recently Launder, Reece, Rodi [3] and Lumley [11]. It is easy to show that the rapid term can be written as (Appendix A)

$$\phi_{ik,2} + \phi_{ki,2} = U^{*m}_{,r} \left(a^{r}_{mik} + a^{r}_{mki}\right)$$

where

$$U^{*m}_{,r} = \bar{U}^{m}_{,r} + \varepsilon^{m}_{pr}\Omega^{p} \quad \text{and} \quad a^{r}_{mik} = -\frac{1}{2\pi}\iiint_{vol} \left(u'_{l}{}^{r}u'_{i}\right)_{,m_l k} \frac{dV'_l}{||\vec{\xi}||} \tag{8}$$

Equation 8 is a rigorous consequence of equation 6 when all second derivatives of the mean velocity are negligible and the turbulence field is homogeneous. It is of course only approximately true in more general flows.

In the case of a cartesian coordinate system, Rotta [10] has commented that the fourth order tensor $a_{r_{mik}}$ should satisfy the following conditions:

symmetry: $a_{rmik} = a_{imrk}$; $a_{rmik} = a_{rkim}$ (9a)

incompressibility: $a_{rmii} = 0$ (9b)

normalization: $a_{rikk} = 2\overline{u'_r u'_i}$ (9c)

isotropic turbulence: $a_{rmik} = (4\,\delta_{il}\delta_{rm} - \delta_{ri}\,\delta_{mk} - \delta_{rk}\,\delta_{mi})\frac{k}{15}$ (9d)

The spectrum of the Reynolds stress completely determines the form of a_{rmik}. If we assume that the spectrum has an equilibrium form, we may expect the form of this fourth order tensor to be expressible in terms of the Reynolds stresses. There are 10 linearly independent combinations of the anisotropy tensor which satisfy the symmetry conditions, incompressibility, normalization, and isotropy condition. In practice, the first two linear terms are used [11]. However, Lumley has shown that this approximation does not satisfy the realizability condition. It is necessary to go at least to second order terms before this can be achieved. A model is said to be realizable if it guarantees that quantities which should be non-negative (like variances) will remain non-negative, and that correlation coefficients will never exceed unity in absolute value.

Lumley's Model [11]

$$I_{rmik} = -(b_{ri}\delta_{mk} - \delta_{ri}b_{mk})/3 + (4\delta_{ri}\delta_{mk} - \delta_{rm}\delta_{ik} - \delta_{rk}\delta_{mi})/30$$
$$+ c(b_{rm}\delta_{ik} + b_{im}\delta_{rk} + b_{rk}\delta_{im} + b_{ik}\delta_{rm} - \frac{11}{3} b_{ri}\delta_{mk} - \frac{4}{3} \delta_{ri}b_{mk}) \qquad (10)$$

with

$$b_{ri} = \frac{\overline{u'_r u'_i}}{q^2} - \frac{1}{3}\delta_{ri} \quad \text{and} \quad a_{rmik} = 2kI_{rmik}$$

and only one constant to adjust.

Launder, Reece and Rodi's Model [3]

These authors approximated the tensor a_{rmik} by a linear combination of Reynolds stresses. Their method is very similar to Lumley's; the symmetry constraints imply that the fourth order tensor may be written as:

$$a_{rmik} = E\delta_{km}\,\overline{u'_r u'_i} + F(\delta_{ki}\,\overline{u'_r u'_m} + \delta_{mi}\,\overline{u'_r u'_k} + \delta_{kr}\,\overline{u'_i u'_m} + \delta_{mr}\,\overline{u'_i u'_k}) + C_2\delta_{ri}\,\overline{u'_k u'_m}$$

$$+ G\,\delta_{ri}\delta_{km}k + H(\delta_{ki}\delta_{mr} + \delta_{mi}\delta_{kr})k \qquad (11)$$

where E, F, G, C_2 are constants. The application of equations 9b and 9c enables four of these constants to be expressed in terms of the fifth: in terms of C_2

$$E = \frac{4C_2 + 10}{11} \quad ; \quad F = -\frac{2 + 3C_2}{11}$$

$$G = -\frac{50C_2 + 4}{55} \quad ; \quad H = \frac{20C_2 + 6}{55}$$

In cartesian coordinates, equation 8 may be then written in the following compact form: (Launder, Reece, Rodi [11]; Cousteix, Aupoix [13])

$$\phi_{ik,2} + \phi_{ki,2} = -\frac{C_2 + 8}{11}\left\{P^*_{ik} - \frac{2}{3}\,\delta_{ik}P^*\right\} - \frac{30C_2 - 2}{55}\,k\left\{\frac{\partial U^*_i}{\partial x_k} + \frac{\partial U^*_k}{\partial x_i}\right\}$$

$$- \frac{8C_2 - 2}{11}\left\{D^*_{ik} - \frac{2}{3}\,\delta_{ik}\,P^*\right\} \qquad (12)$$

with

$$P^*_{ik} = -\overline{u'_i u'_j}\,\frac{\partial U^*_k}{\partial x_j} - \overline{u'_k u'_j}\,\frac{\partial U^*_i}{\partial x_j} \quad ; \quad D^*_{ik} = -\overline{u'_i u'_j}\,\frac{\partial U^*_j}{\partial x_k} - \overline{u'_k u'_j}\,\frac{\partial U^*_j}{\partial x_i}$$

$$P^* = -\overline{u'_i u'_k}\,\frac{\partial U^*_k}{\partial x_i} \quad ; \quad \frac{\partial U^*_k}{\partial x_i} = \frac{\partial \bar{U}_k}{\partial x_i} + \varepsilon_{kpi}\,\Omega^p$$

It is interesting to note that equation 12 has been derived mainly from kinematic arguments, for the case of isotropic turbulence subjected to sudden distortion, equation 12 reduces to:

$$(\phi_{ik} + \phi_{ki})_2 = .4k\left(\frac{\partial \bar{U}_i}{\partial x_k} + \frac{\partial \bar{U}_k}{\partial x_i}\right) \qquad \text{irrespective to the constant } C_2$$

which is the exact result derived by Crow [9].

However, it appears that equation 11 together with relations 9 cannot be generalized to any kind of coordinate system. In fact, if we go back to equation 8 it is easy to show that the fourth order a^r_{mik} does not satisfy conditions 9b and 9c. A detailed analysis is then necessary to derive a general formulation for relation 8. While we await the final resolution of this problem (the study is under development), it is interesting to point out some features of this problem.

It appears from equations 10 and 12 that the "rapid term" of the pressure strain correlation might be expressed in terms of the Reynolds stresses or the anisotropy tensor and what we will call here the "external effects", e.g. mean strain rate, rotation. Moreover, one of the essential properties of the pressure strain correlation is its character of redistributivity (e.g. this term vanishes under contraction of indices). It also turns out, looking at equation 12, that the "rapid part" of the pressure strain correlation, is a turbulence production like term, e.g. the term may be approximated by a similar expression to the production by the turbulence through the "external effects."

Then a simple way to express the "rapid term" may be given as follows:

$$\phi_{ik,2} + \phi_{ki,2} = C_p(P^*_{ik} + \frac{2}{3} P^*\delta_{ik}) \tag{13}$$

where

$$P^*_{ik} = -\overline{u'_i u'^j}\, U^*_{k,j} + \overline{u'_k u'^j}\, U^*_{i,j}$$

$$P^* = -\overline{u'_i u'^k}\, U^{*i}_{,k} \quad \text{and} \quad U^{*i}_{,k} = \bar{U}^i_{,k} + \varepsilon^i_{pk}\Omega^p$$

In order to be sure that the expression will behave properly in all coordinate systems, it is necessary that the constant be a function of the invariants of the anisotropy tensor, and the local Reynolds number of the turbulence. These invariants are defined as:

$$II = -\frac{b_i^k b_k^i}{2} \quad ; \quad III = \frac{b_i^j b_j^k b_k^i}{3} \tag{14}$$

A formulation of the coefficient C_p is under survey, some directions towards this end have been proposed by Lumley [11].

According to equation 13, $\phi_{ik,2} + \phi_{ki,2}$ tends to isotropize the turbulence production tensor. However, it is interesting to note that if the production due to the mean strain is following this trend, it is not true for the terms involving the Coriolis force effects.

1.2.2 Modelling of $\phi_{ik,1}$: "Return to Isotropy"

Let us first present some basic features about this term:

$$\phi_{ik,1} = \frac{1}{4\pi} \iiint_{vol} \overline{(u'_l u'_l{}^m)_{,\ell m} u'_{i,k}} \frac{dV'}{||\vec{\xi}||}$$

$$\phi_{ki,1} = \frac{1}{4\pi} \iiint_{vol} \overline{(u'_l u'_l{}^m)_{,\ell m} u'_{k,i}} \frac{dV'}{||\vec{\xi}||} \tag{15}$$

This term involves only the fluctuating quantities and is responsible for the return of anisotropic turbulence to isotropy, in the absence of other disturbing effects. Rotta [10] pointed out that $\phi_{ik,1} + \phi_{ki,1}$ is a symmetric tensor with zero trace, which vanishes if the turbulence is isotropic. Since this term acts to interchange energy among the components when the turbulence is anisotropic, and vanishes when it is isotropic, it is natural to express it in terms of the anisotropy tensor of the turbulence, which is also a symmetric second rank tensor which vanishes if the turbulence is isotropic. It is also easy to show that, for a flow without mean strain and rotation and initially non isotropic the Reynolds stress equation may be written as (cartesian tensors)

$$\frac{\partial \overline{u_i' u_k'}}{\partial t} = \phi_{ik,l} + \phi_{ki,l} - \frac{2}{3}\delta_{ik}\varepsilon$$

which leads to

$$\frac{\partial(\overline{u_i' u_k'} - 2/3\ \delta_{ik} k)}{\partial t} = \phi_{ik,l} + \phi_{ki,l}$$

Therefore, as the flow must return to an isotropic state, the following assumption is made:

$$\phi_{ik,l} + \phi_{ki,l} = -C_1 \frac{\varepsilon}{k}\left(\overline{u_i' u_k'} - \frac{2}{3}\ \delta_{ik}\ k\right) \qquad (16)$$

where $\frac{k}{\varepsilon}$ is the rate of time at which the energy is mainly transmitted from big eddies to dissipative ones. The value of the constant has been originally set to about 1.4 by Rotta. Different authors have then used a value of C_1 of about 1.5.

According to equation 16, the sign of $\phi_{ik,l} + \phi_{ki,l}$ is always such as to promote a change towards isotropy, its magnitude being proportional to the local level of anisotropy. This term is called "return to isotropy" term, and this model gives acceptable behavior in most situations of practical importance. However, it does not take into account the variation of the coefficient C_1 with the local Reynolds number of turbulence, or the variation with anisotropy. It is found experimentally that C_1 is larger when the turbulence is more anisotropic. Consequently, the coefficient C_1 appears to be a function of the Reynolds number and of the anisotropy. This anisotropy is generally created by "external effects", such as shape of the boundaries, rotation, mean strain. In fact, these effects mainly influence the time of return to isotropy. Then we may write that the tensor $\phi_{ik,l} + \phi_{ki,l}$ is a functional of the anisotropic tensor, but also depends on the Reynolds number, the "external effects" explicitly. In fact, we

may divide these effects in three main categories:

the gross turbulent structure effects: through anisotropic tensor

the dissipative effects: through Reynolds number of turbulence

the "external effects": through mean strain, rotation, curvatures

It is shown in Lumley [11] that, even though in many flows the turbulence does not become sufficiently anisotropic to make realizability a necessary condition, there are, however, some situations where the turbulence does become nearly two dimensional. The constant C_1 should then reduce to 1. It is clear that in order to be sure that the expression will behave properly in all corodinate systems and situations, it is necessary that C_1 be a function of the invariants of the anisotropy tensor, the Reynolds number and the "external effects".

Lumley [11] proposed a formulation of the constant C_1. In his paper the constant is $2C_1$. Then the formulation is:

$$2C_1 = C_2 = 2 + F(R_\ell, II, III)(1/9 + 3III + II) \tag{17}$$

where $R_\ell = \overline{q^2}^2/9\varepsilon\nu$ and II and III are the invariant of the anisotropic tensor.

F is then expressed as

$$F = \exp(-7.77/R_\ell^{1/7})\{72/R_\ell^{1/2} + 80.1\ \mathrm{Ln}[1 + 62.4\ (-II + 2.3\ III)]\} \tag{18}$$

Equation 18 is simply an interpolation formula to connect the known value in a certain number of experiment. However, this proposition gives certain directions which could be followed to establish a formulation of the constant C_1.

$$C_1 = C_1(R_T, II, III, R_{ic}) \tag{19}$$

where R_T is the local Reynolds number and R_{ic} is the local Richardson

number of the rotation. The formulation of the quantity C_1 is under survey. It is not known now whether all these effects are really necessary to be taken in account. However, it is certain that the Reynolds number is to be important in the evolution of the coefficient C_1. At this stage arguments concerning the expansion of C_1 in a power series remains one of the directions to follow to derive an expression for the coefficient.

1.2.3 Modelling Near the Wall

Near the wall, the surface integral in equation 5 appears to become important in magnitude and must not be neglected. In fact, Bradshaw [14] demonstrated that the surface integrals ζ_{ik} and ζ_{ki} would make a significant contribution to the pressure-strain correlation as long as the typical size of the energy containing eddies was of the same order as the distance from the wall. As he remarked, this condition is always satisfied in near wall flows.

If we refer to Launder, Reece, Rodi [3], for a plane wall (with x_2 normal to the surface) the pressure strain correlation may be recast in the following form, from which the surface integral is eliminated:

$$\overline{\frac{p'}{\rho}\frac{\partial u_i'}{\partial x_k}} = \frac{1}{4\pi}\int_{vol}\left\{\overline{\left(\frac{\partial^2 u_\ell' u_m'}{\partial x_\ell \partial x_m}\right)_1}\frac{\partial u_i'}{\partial x_k} + 2\left(\frac{\partial \bar{U}_j}{\partial x_2}\right)_1\overline{\left(\frac{\partial u_2'}{\partial x_1}\right)_1\frac{\partial u_i'}{\partial x_k}}\right\}\left(\frac{1}{|x-y|}+\frac{1}{|x-y^*|}\right)dv \tag{20}$$

where y* is the image of the point Y in regard to the wall.

This form again suggests that there should be two contributions to the near-wall effect corresponding to the reflecting wall influence of $\phi_{ik,1}$ and $\phi_{ik,2}$. Therefore, they proposed a formulation of the wall proximity effect on the pressure strain term as follows:

$$(\phi_{ik} + \phi_{ki})_w = \{C_1 \frac{\varepsilon}{k} (\overline{u'_i u'_k} - \frac{2}{3} \delta_{ik} k) + \frac{\partial \bar{U}_\ell}{\partial x_m} (b^{mi}_{\ell k} + b^{mk}_{\ell i})\} F(\frac{\ell}{x_2}) \qquad (21)$$

where ℓ denotes the length scale of the energy containing eddies, thus

$$F(\frac{\ell}{x_2}) = \frac{k^{3/2}}{\varepsilon x_2}$$

In the general case, the two surface integrals are:

$$\zeta_{ik} = \frac{1}{4\pi\rho} \int_S \{\frac{1}{||\vec{\xi}||} \overline{\frac{\partial p'_1}{\partial n_1} u'_{i,k}} - \overline{p'_1 u'_{i,k}} \frac{\partial^1 / ||\vec{\xi}||}{\partial n_1}\} ds \qquad (22a)$$

$$\zeta_{ki} = \frac{1}{4\pi\rho} \int_S \{\frac{1}{||\vec{\xi}||} \overline{\frac{\partial p'_1}{\partial n_1} u'_{k,i}} - \overline{p'_1 u'_{k,i}} \frac{\partial^1 / ||\vec{\xi}||}{\partial n_1}\} ds_1 \qquad (22b)$$

where the quantities with subscript 1 correspond to point p_1 and others to point p. $\partial/\partial n_1$ is the normal derivative and dS_1 is a surface element. The value of this integral is to be evaluated at point p. Following Raj [15], a series expansion would indicate that, to a first order approximation, equation 22a can be written as:

$$\zeta_{ik} = \frac{1}{4\pi ||\vec{\xi}||} \overline{u'_{i,k} \int_s \frac{\partial p'_1}{\partial n_1} ds} = F_{ik} \{\text{deviatoric, external effects}\} \qquad (23)$$

It is clear that near the wall the deviatoric of the Reynolds stress and the "external effects" should have some contribution to the surface integrals.

Unfortunately, the experimental results very near the wall are extremely rare, particularly on curved surfaces, and it is therefore very difficult to derive a specific modelling of the surface integral in the case of highly curved flows. However, for flows over mildly curved surfaces we may hope that the only important length scales are the local turbulen t length scale $\frac{k^{3/2}}{\varepsilon}$ and the normal distance to the wall y. Moreover, it is also hoped that the predictions will be less sensitive to assumptions made to third order correlations, handling the second order ones exactly. Then, following an analysis close to Launder, Reece and Rodi's one, the effect of

the surface integral is modelled through the introduction of a function of the turbulence length scale and the normal distance to the wall y, in the general model for $(\overline{pu'_{i,k} + pu'_{k,i}})$.

$$\frac{\overline{p'u'_{i,k} + p'u'_{k,i}}}{\rho} = \{-C_1 \frac{\varepsilon}{k} (\overline{u'_i u'_k} - \frac{2}{3} \delta_{ik} k) - C_p (P^*_{ik} - \frac{2}{3} \delta_{ik} P^*)\} f(\frac{\ell}{n_i x^i}) \quad (24)$$

where $F(\frac{\ell}{n_i x^i})$ must reduce to one away from the wall.

1.2.4 Summary

A model for the pressure strain correlation has been proposed, which includes the effects of rotation and curvature explicitly. However, this model is still under study as three functions C_1, C_p and $F(\frac{\ell}{n_i x^i})$ have to be defined. Some directions have been given, but further work is needed.

The pressure strain correlation model is presented above (equation 24). The coefficients C_1 and C_p are functions of the local Reynolds number, the Richardson number and the invariants of the deviatoric of the Reynolds stress tensor, while $F(\frac{\ell}{n_i x^i})$ is function of the length scale and the normal distance to the wall.

1.3 Dissipative Terms and Diffusion

Referring to equation 1 for Reynolds stress, two kinds of terms remain to be modelled--the diffusion term, which included viscous terms as well as pressure velocity correlations and triple velocity correlation, and the dissipation terms. Let us examine the dissipative terms.

Dissipative Terms

$$D = -\overline{F_k^j u'_{i,j}} - \overline{F_i^j u'_{k,j}} \quad \text{where} \quad F_{ij} = \mu(u_{i,j} + u_{j,i}) = 2\mu S_{ij} \tag{25}$$

in incompressible flows, only the fluctuating quantities remain in equation 25 then,

$$D = -\mu\left(\overline{S'^j_k u'_{i,j}} + \overline{S'^j_i u'_{k,j}}\right) \quad \text{where} \quad S'_{ij} = \frac{1}{2}\left(u'_{i,j} + u'_{j,i}\right) \tag{26}$$

Terms like $\overline{s'^j_k u'_{i,j}}$ and $\overline{s'^j_i u'_{k,j}}$ have been derived in the previous report and it has been shown that we may write:

$$\overline{s'^j_k u'_{i,j}} \approx \frac{\varepsilon}{3\nu}\left\{\delta_{ik} + a_1 \sqrt{\frac{\nu}{\varepsilon}}\,\overline{s_{ik}}\right\} \tag{27a}$$

$$\overline{s'^j_i u'_{k,j}} \approx \frac{\varepsilon}{3\nu}\left\{\delta_{ik} + a_2 \sqrt{\frac{\nu}{\varepsilon}}\,\overline{s_{ik}}\right\} \tag{27b}$$

Therefore equation 26 may be approximated by

$$D = -\rho\varepsilon\,\frac{2}{3}\left\{\delta_{ik} + a\sqrt{\frac{\nu}{\varepsilon}}\,\overline{s_{ik}}\right\} \tag{28}$$

A dimensional analysis, using similar approximations as the ones used in the previous report shows that the term involving the mean strain is of order $R_e^{-1/2}$, and therefore is negligible in high Reynolds number flows. In that case the decay rate D reduces to:

$$D = -\frac{2}{3}\,\delta_{ik}\,\rho\varepsilon \tag{29}$$

which is the form proposed by Launder, Reece and Rodi [3] who assume the dissipative motions to be isotropic. Several experimental studies have shown that turbulence does not remain locally isotropic in the presence of strong strain fields [8, 16]. Nevertheless, equation 29 seems to be enough for most of the flows studied by Launder et al. In the case of low Reynolds

number flows, the energy containing and dissipation range of motions overlap and the dissipation rate is then commonly approximated as [10]

$$-D = \rho \frac{\overline{u_i' u_k'}}{k} \varepsilon \tag{30}$$

Equations 29 and 30 have led a number of workers to propose that in general the correlation may be approximated as:

$$D = -\frac{2}{3} \rho\varepsilon \left\{(1 - F_s)\delta_{ik} + \frac{\overline{u_i' u_k'}}{2/3\ k} F_s\right\} \tag{31}$$

where F_s is a function of the turbulent Reynolds number $R_T = \frac{k^2}{\nu\varepsilon}$.
A detailed analysis of equation 31 has been proposed by Hanjalic and Launder [17]. However, equation 30 is not asymptotically valid. In fact, as the Reynolds number increases the equation 30 should reach continuously the form obtained for very high Reynolds number (equation 29). It seems that equation 28 should not present this problem, therefore we may re-write equation 28, including the Reynolds number of the turbulence

$$D = -\frac{2}{3} \rho\varepsilon\left\{\delta_{ik} + a\ \frac{k}{\varepsilon} \overline{s}_{ik} R_T^{-1/2}\right\} \tag{32}$$

where a is a constant of order 1. Some numerical calculations are needed to derive an "exact" value for the constant a.

Diffusion Terms

There are two kinds of "diffusion" terms, the viscous ones and the third order correlation ones. The diffusion terms in equation 1 are:

$$\text{Dif} = -\underbrace{\left(\overline{p' u_i'}\delta_k^j + \overline{p' u_k'}\delta_i^j + \rho\overline{u_i' u_k' u^j}\right)_{,j}}_{\text{triple correlation}} + \underbrace{\left(\overline{u_i' F_k^j} + \overline{u_k' F_i^j}\right)_{,j}}_{\text{viscous}}$$

A dimensional analysis, again shows that the viscous terms are of order R_e^{-1} and smaller than other terms. Therefore, it is evident that these terms will be important only for low Reynolds number flows, very near a wall. The triple correlation terms need to be modelled so that the complete set of Reynolds stress equations is closed. This work is presently under survey.

2. TURBULENCE MODELLING: k-ε MODEL

2.1 Introduction

An analysis of the kinetic energy and the dissipation equations have been presented in the previous report [1]. At that time, we made the following remarks.

The rotation does not appear explicitly in the kinetic energy equation, but is present in the dissipation equation. However, in high Reynolds number flows, we have shown that this explicit effect was negligible. At low Reynolds number (the Reynolds number is based on the following turbulence characteristics: k, ε and is $k^2/\nu\varepsilon = R_T$), the dissipation becomes non-isotropic and both the effects of Reynolds number and Richardson number may be important in this case. But the main remark is that the effects of rotation are more important on the production of turbulence implied by the interaction of the Reynolds stresses and the "external effects", than on the others. In fact, if we refer to the previous chapter it is easy to see that the Reynolds stresses may be greatly affected by the rotation while the kinetic energy and its dissipation rate are not so much affected. Then, it appears that in any two-equation turbulence model combined with an eddy viscosity hypothesis, the first priority is to control the calculation of the eddy viscosity coefficient. In fact, in most of the work done, the main hypothesis to derive the viscosity law assumes that the turbulent viscosity is isotropic. For simple shear flows, this gives adequate results at very low cost. However, for three dimensional flows and particularly for some boundary layer flows the velocity vector $\vec{u}$ and $\vec{\nabla u}$ are not aligned in general. Therefore the isotropic eddy viscosity is not adapted to predict the behavior of the Reynolds stresses. Solving the complete set of Reynolds

stress equations would avoid this difficult problem, but it is a tremendous work which involves very important numerical schemes, which are only in their early stages of development. On the other hand, the eddy viscosity is a fourth order tensor in general, however, in many real flow situations, there are only two directions in the flows which are of equal importance (it is the case for blade boundary layers). Therefore, we are able to derive different eddy viscosities to take account for the anisotropy of the flow. More generally, it would be interesting to classify the flows that the engineer is encountering in which we could use such an eddy viscosity model. This can be related to "Zonal Modelling" referred to by Kline during the last Stanford Conference on complex turbulent flows.

To be able to check some of the assumptions made previously, particularly for low Reynolds number modelling, a computer code was developed based on the Patankar-Spalding procedure [18], which solves the parabolic two-dimensional and quasi-three dimensional transport equation for the velocity, the kinetic energy and the dissipation. Chapter 2 is divided into two parts. In the first part, we present some simple approach to the modelling of the different stresses. In the second part, some calculations of a boundary layer developing on a rotating and non-rotating cylinder is presented. The non-rotating cylinder calculation has been done to show the effects of the corrections due to Reynolds number and Richardson number of rotation in the dissipation equation. A brief explanation of the Patankar-Spalding numerical method is given in Appendix B.

2.2 Algebraic Modelling of the Reynolds Stresses

The Reynolds stress equation presented in Chapter 1 (equation 1), together with the assumptions made, may be written as:

$$(\rho \dot{\overline{u_i'u_k'}}) + (\rho \overline{u_i'u_k'} \bar{U}^j)_{,j} = -(\overline{p'u_i'}\delta_k^j + \overline{p'u_k'}\delta_i^j + \rho\overline{u_i'u_k'u^j} - \overline{u_i'F_k^j} - \overline{u_k'F_i^j})_{,j} + \zeta(\overline{u_i'u_k'}) \tag{33}$$

where the left hand side is the convective like term, the first group of the right hand side is the diffusion like term and $\zeta(\overline{u_i'u_k'})$ is the source-sink term.

$$\frac{\zeta(\overline{u_i'u_k'})}{\rho} = P_{ik}\left[1 - C_p F\left(\frac{\ell}{n_i x^i}\right)\right] + R_{ik}\left[1 - \frac{C_p F}{2}\left(\frac{\ell}{n_i x^i}\right)\right] + \frac{2}{3}\delta_{ik}\left[C_p F\left(\frac{\ell}{n_i x^i}\right)P - \varepsilon\left(1 - C_1 F\left(\frac{\ell}{n_i x^i}\right)\right)\right] - C_1 F\left(\frac{\ell}{n_i x^i}\right)\varepsilon\frac{\overline{u_i'u_k'}}{k} - \frac{2}{3}\frac{a}{R_T}\, k\, s_{ik} \tag{34}$$

where

$$P_{ik} = -\overline{u_i'u'^j}\,\bar{U}_{k,j} - \overline{u_k'u'^j}\,\bar{U}_{i,j} \quad ; \quad R_{ik} = -2\Omega^p(\varepsilon_{ipj}\,\overline{u_k'u'^j} + \varepsilon_{kpj}\,\overline{u_i'u'^j})$$

$$P = -\overline{u_i'u'^j}\,\bar{U}^i_{,j} \quad ; \quad S_{ik} = \frac{1}{2}(\bar{U}_{i,k} + \bar{U}_{k,i})$$

The kinetic energy equation may be deduced from equation 33.

$$(\dot{\rho k}) + (\rho k\bar{U}^j)_{,j} = -(\overline{p'u_i'}\,\delta^{ij} + \overline{\rho ku'^j} - \overline{u_i'F^{ij}})_{,j} + \zeta(k) \tag{35}$$

where $\zeta(k)$ is the source-sink term and $k = \frac{1}{2}\,g^{ik}\,\overline{u_i'u_k'}$

$$\frac{\zeta(k)}{\rho} = P - \varepsilon \tag{36}$$

The transport and diffusion terms are treated by the technique known as algebraic stress modelling [19]. The net transport of $\overline{u_i'u_k'}$ is assumed to be locally proportional to the net transport of k, the coefficient of proportionality taken as $\overline{u_i'u_k'}/k$. Thus for incompressible flows,

$$(\overline{u_i'u_k'})\dot{}+(\overline{u_i'u_k'}\,\bar{U}^j)_{,j} - \mathrm{Dif}(\overline{u_i'u_k'}) = \frac{\overline{u_i'u_k'}}{k}\left(\dot{k} + (k\bar{U}^j)_{,j} - \mathrm{Dif}(k)\right) \qquad (37)$$

where Dif denotes diffusion terms.

This treatment appears to be reasonably accurate for thin shear layers except near an axis of symmetry. However, the turbulent boundary layers in a rotor are far to be axisymmetric and more over if any symmetry exists it must be a symmetry in regard to the axis of rotation which is never in "contact" with the fluid. Therefore, substitution of the model assumptions yields the following algebraic equation for the Reynolds stresses:

$$\frac{\overline{u_i'u_k'}}{k} = \frac{2}{3}\delta_{ik} + \frac{R_{ik}\left(1 - \frac{C_p}{2}F\left(\frac{\ell}{x^i n_i}\right)\right)+\left(1 - C_p F\left(\frac{\ell}{n_i x^i}\right)\right)\left(P_{ik} - \frac{2}{3}\delta_{ik}P\right) - \frac{2}{3}\,a\,R_T^{-1/2}\,k\,S_{ik}}{P + \varepsilon\left(C_1 F\left(\frac{\ell}{n_i x^i}\right) - 1\right)} \qquad (38)$$

The form of the wall-damping function $F\left(\frac{\ell}{n_i x^i}\right)$ must now be specified, as well as the values of the coefficients C_p and C_1, and a. This is presently under survey, however, we still may discuss equation 38. This equation is basically a non-linear algebraic system of six equations, in fact, which have to be solved simultaneously. The six equations plus a formulation for the dissipation rate, will form a closed system, providing we know the mean flow.

It is interesting to note that several authors have treated similar equations as a linear system, provided that the kinetic energy k and dissipation rate ε are calculated with two differential equations, and most of all the computations are restricted to local equilibrium turbulence for which P/ε is unity.

In this case, equation 38 provides mainly some indications on the anisotropy of the flow and then the quantitative values are given through the calculation of k and ε. It is therefore not necessary to define any eddy

viscosity formulation. If we want to solve this system still linearly, when P/ε is a function of the space, it is necessary to make an assumption on the denominator in equation 38; then provided that the evolution of the stresses in the main direction of the flow is not very important, which is a good approximation in boundary layers flows, we may calculate the stresses, supposing that $P + \varepsilon\left(C_1 F \left(\frac{P}{n_i x^i}\right) - 1\right)$ is taken at the previous step, in a parabolic marching method, where all the quantities are known.

On the other hand, it is also possible to solve the system of six non-linear equations plus the equation for the dissipation simultaneously. The number of equations to solve is then reduced to seven. However, it is well known that non-linear systems are very much sensitive to the initial conditions we must give in order to iterate and converge toward the solution. But still, in the case of parabolic type flows, the evolutions in the stream-wise direction are very much less important than in the normal plane, so that it is possible to use the values at the previous step as a first guess, and as the changes should be small, the process should converge rapidly.

2.3 Calculation of the Boundary Layer Over an Axial Cylinder

The governing equations in the axial and circumferential directions for a uniform property, axisymmetric turbulent boundary layer flow may be written:

$$\rho\bar{U}\frac{\partial\bar{U}}{\partial x} + \rho\bar{V}\frac{\partial\bar{U}}{\partial y} = -\frac{\partial\bar{p}}{\partial x} + \frac{1}{r}\frac{\partial r\left(\mu\frac{\partial u}{\partial y} - \rho\overline{u'v'}\right)}{\partial y}$$

$$\rho\bar{U}\frac{\partial r\bar{W}}{\partial x} + \rho\bar{V}\frac{\partial r\bar{W}}{\partial y} = \frac{1}{r}\frac{\partial\left(r^3\mu\frac{\partial\bar{W}/r}{\partial y} - r^2\rho\overline{v'w'}\right)}{\partial y} \qquad (39)$$

which together with the continuity equation

$$\frac{\partial r\bar{U}}{\partial x} + \frac{\partial r\bar{V}}{\partial y} = 0$$

and of radial equilibrium of the mean motion

$$\frac{\partial \bar{p}}{\partial y} = \rho \frac{\bar{W}^2}{r}$$

Constitute a closed set if we define a model for the two Reynolds stresses $\rho\overline{uv}$ and $\rho\overline{w'v'}$. The independent variables x and y are respectively the axial and radial direction. The corresponding velocities are $\bar{U}$ and $\bar{V}$. W denotes the circumferential velocity and is zero for non rotating cylinder. All symbols are defined in the nomenclature. The effective viscosity of this flow may be taken as the sum of the laminar and turbulent contributions, i.e.

$$\mu_{eff} = \mu + \mu_T$$

Provided that the two Reynolds stresses are respectively aligned with the correspondent mean strain. The turbulent viscosity μ_T is obtained from the solution of the following differential equations.

Turbulent kinetic energy k:

$$\rho\bar{U}\frac{\partial k}{\partial x} + \rho\bar{V}\frac{\partial k}{\partial y} = \frac{1}{r}\frac{\partial r\left(\mu + \frac{\mu_T}{\sigma_k}\right)\frac{\partial k}{\partial y}}{\partial y} + P - \rho\varepsilon - 2\mu\left(\frac{\partial k^{1/2}}{\partial y}\right)^2 \qquad (40)$$

Dissipation rate ε:

$$\rho\bar{U}\frac{\partial \varepsilon}{\partial x} + \rho\bar{V}\frac{\partial \varepsilon}{\partial y} = \frac{1}{r}\frac{\partial r\left(\mu + \frac{\mu_T}{\sigma_\varepsilon}\right)\frac{\partial \varepsilon}{\partial y}}{\partial y} + C_{\varepsilon_1}\frac{\varepsilon}{k}P - C_{\varepsilon_2}\rho\frac{\varepsilon^2}{k} + C_{\varepsilon_3}\nu P^{1/2} \qquad (41)$$

with

$$P = -\rho\overline{u'v'}\frac{\partial U}{\partial y} - \rho\overline{w'v'}\left(\frac{\partial \bar{w}}{\partial y} - \frac{\bar{w}}{r}\right)$$

$$\mu_T = C_\mu F_\mu \rho\frac{k^2}{\varepsilon} \quad , \quad F_\mu = \exp\left(-3.4/(1 + R_T/50)^2\right) \quad , \quad R_T = \frac{k^2}{\nu\varepsilon}$$

$$\sigma_k = 1 \quad , \quad \sigma_\varepsilon = 1.3 \quad , \quad C_{\varepsilon_1} = 1.44 \quad , \quad C_{\varepsilon_2} = 1.92\left(1 - .3\exp(-R_T^2)\right)$$

$$C_{\varepsilon_3} = 2 \quad \text{and} \quad \rho\overline{u'v'} = \mu_T \frac{\partial \bar{U}}{\partial y} \quad , \quad \rho \frac{\overline{w'v'}}{r} = \frac{\mu_r}{\sigma_w} \frac{\partial \bar{W}/r}{\partial y} \tag{42}$$

Discussion about the coefficient σ_w will be presented later. In the preliminary calculations σ_w has been taken equal to 1. This coefficient represents the anisotropy existing between the Reynolds stress components and the mean strain components. This model has been tested first, on an axisymmetric cylinder to check the effects of the corrections due to low Reynolds on the equation of dissipation rate ε, through the coefficient C_{ε_2}. We may see on Figure 1 that the correction allows a 30 percent damping of the value of ε. However this damping function starts to be effective at Reynolds numbers lower than two which means that occurs well inside the viscous sublayer where the viscous effects are preponderant over the turbulent ones. In Figures 2 to 6 we present some comparison between two calculations, the first one using the low Reynolds damping function in the equation of ε and the second one letting $C_{\varepsilon_2} = 1.92$. It appears that the maximum differences around 1 percent on quantities such as the kinetic energy, the dissipation rate, the wall shear stress and below 1 percent for the velocity profile, which is well beyond the accuracy we may hope from this type of calculation and experimental measurements of these quantities. We may wonder why then implement such corrections. It is possible in certain very low turbulence flows that this function may have some more important effects. However it is evident that again the changes due to the production terms in equation 40 and 41 are much more important and over a wider distance from the wall. Then it is in fact the modelling of the Reynolds stresses themselves which is making the big difference.

To illustrate this, the calculation of the boundary layer developing over a cylinder of which one part is rotating is a good test case. In fact, the boundary layer first develops along the static cylinder as a classical

two dimensional boundary layer. It is then submitted to a sudden transversal distortion by rotation of the downstream part of the cylinder. Sufficiently far away the origin of the spinning part, the reorganization of the three-dimensional boundary layer into a two-dimensional one, in a relative coordinate system is in an advanced phase. Very near the discontinuity in boundary conditions, the three dimensionality is stronger. A recent paper of Arzoumanian et al. [25] shows that in a relative coordinate system linked to the moving cylinder, far from the origin of the spinning part, the turbulent quantities are very slightly influenced by the three-dimensional effects, except the Reynolds stress $\overline{uv}$. This suggests that the evolution of $\overline{uv}$ and $\overline{wv}$ in the fixed coordinate system are different and therefore the anisotropy of the Reynolds stress tensor is quite important, at least in the very beginning of the rotation. Then a model based on an isotropic eddy viscosity (e.g. the two directions have the same characteristics) should fail to represent the dynamic characteristic of such a flow.

We present hereafter some calculations of the rotating cylinder with an isotropic eddy viscosity to illustrate our purpose. The calculation is confronted to the experimental results of Lohmann [20]. Figures 7 and 8 show the development of the mean velocity profiles U and W, while Figure 9 shows the evolution of the limiting streamline angle along the streamwise direction. Differences between the experimental and calculated profiles are up to 9 percent in our calculation, it can be easily seen in Figure 7.

However, larger differences appear in the calculation of the Reynolds stresses $\overline{u'v'}$ and $\overline{w'v'}$, (Figures 10 and 11) particularly for $\overline{w'v'}$. It is then evident from these calculations that the isotropic eddy viscosity fails to represent the characteristics of the flow.

Different authors have proposed some alternative to model such a behavior. For example, Koosilin and Lockwood [21] derived eddy viscosities for the two directions and then define a viscosity ration $\sigma_{1,2} = \mu_{T_1}/\mu_{T_2}$ which globally represent the anisotropy of the Reynolds stresses. Cousteix et al. [22] proposed a similar approach with the k-ε model.

A very simple way of deriving two different eddy viscosities is to use equation 38, which gives the ratio $\overline{u'v'}/\overline{w'v'}$ representing the differences between these two Reynolds stresses.

We are now developing two different schemes using equation 38 to solve the turbulent field. The first scheme solves the momentum equations and the kinetic energy and dissipation rate equations first using the stresses $\overline{u'v'}$ and $\overline{v'w'}$ calculated from the linear form of the equation 38 as we discussed previously. The second scheme solves the momentum equations and dissipation equation using again the stresses $\overline{u'v'}$, $\overline{v'w'}$ and $\overline{u'^2}$, $\overline{v'^2}$, $\overline{w'^2}$ calculated from the algebraic nonlinear system 38. The system of six nonlinear equations is solved with the iterative Newton-Raphson scheme.

These two programs are now almost in their achieved form. A brief discussion of the numerical method used to solve the differential equations is presented in Appendix B.

3. NUMERICAL ANALYSIS OF BLADE AND HUB WALL BOUNDARY LAYERS

In the early stages of the present investigation, an attempt was made to predict the blade boundary laver using the parabolized form of the Navier-Stokes equations. The procedure involves the solution of the momentum equations and the Poisson equation for the pressure.

Numerous investigators have tried different ways of deriving and solving the Poisson equation for the pressure. In most of the cases the procedure requires some kind of iteration to ensure mass conservation. All the previous investigations indicated that the solution of the Poisson equation and the ensurance of mass conservation are the most troublesome parts of the whole procedure. The efficiency and accuracy of the method depends almost exclusively on these factors. The situation becomes more difficult in the case of complex geometry, like for example in the case of a turbomachinery rotor passage.

Up to date, nobody has come up with a "clean" solution to the problem and all the evidence shows that coupling the momentum equation with the Poisson equation for the pressure is an ill-posed problem. Based on the above discussion we decided to try to solve the problem by using a procedure which does not involve the solution of a Poisson equation for the pressure.

The first attempt was to solve the incompressible set of equations (three-momentum and continuity) with the vector of unknown given by,

$$g = \begin{pmatrix} P \\ U \\ V \\ W \end{pmatrix}$$

We tried to solve this system of equations by marching in the streamwise direction ξ. We soon realized that:

1. When treating the streamwise pressure gradient fully explicitly (i.e., following the classical assumption of the parabolized Navier-Stokes equations) the Jacobian matrix, which expresses the changes in the streamwise direction, becomes singular.

2. When treating the streamwise pressure gradient partly explicitly and partly implicitly the solution is unstable. This is because our system of equations has both negative and positive eigenvalues. This makes it impossible to solve the system of equations by marching in the streamwise direction.

An attempt is presently being made to solve the compressible set of equations by marching in the streamwise direction. This procedure was developed by Govindan and is described in ref. 24. The code is presently working well, and it has already given very encouraging results for some test cases. So we decided to use that code for the solution of the flow in the blade passage, including the hub wall and the blade boundary layer.

We are presently working to adapt the code to our particular problem with the turbulence closure model described in section 2 of the report.

4. EXPERIMENTAL STUDY OF THE ROTOR BLADE BOUNDARY LAYER IN AN AXIAL FLOW COMPRESSOR ROTOR

The measurement of the blade boundary layer in the rotor of an axial flow compressor is presently being carried out. The study is performed in the Axial Flow Compressor Facility, located in the Turbomachinery Laboratory of the Department of Aerospace Engineering. The only similar study available at the present time is that due to Lakshminarayana et al. [23,24] inside the rotor of an axial flow fan.

All the measurements reported here are taken with a hot-wire probe rotating with the rotor. A miniature cross flow "X" hot-wire probe, TSI 1247, with sensor diameter of 3 μm and sensor length equal to 1 mm is used.

Both the sensors are within a circle of approximate diameter 1.5 mm. The sensors are located in the zR plane with their axis at 45° to the z axis (Fig. 10). The probe is traversed normal to the blade surface. Since the flow traverse is done close to the blade surface, the component of velocity in the n direction is assumed to be small.

The boundary layer measurements are carried at non-dimensionalized radii R = 0.583, 0.67, 0.75, 0.832, 0.918 and at various chordwise locations. Only one chordwise location has been surveyed so far, at each of these radial locations.

4.1 Experimental Results

Only a brief interpretation of the results is given here. Detailed interpretation will be given when the whole set of data is completed.

The streamwise velocity profiles are shown in Figures 11 through 15. At all suction side locations the profiles are relatively well behaved. The profiles on the pressure side at the locations near to the hub (R = 0.583, 0.67) have an unconventional shape. This probably comes from the secondary velocities developed in the hub wall region.

The radial velocity profiles are shown in Figures 16 through 20. At the location nearest to the hub (R = 0.583) the radial velocity is very small (less than 4 percent of U_e). At R = 0.67 a strong radially outward velocity starts to develop very near the surface. At R = 0.75 we see that the radial velocity does not get stronger but it spreads away from the surface (see Figures 18 and 19). At the location nearer to the tip, R = 0.918 (Figure 20), the radial velocity becomes again small. Here the radial velocity is affected by the leakage flow, and the annulus-wall boundary layer.

The streamwise and radial turbulent intensities are shown in Figures 21 through 26. In almost all locations we see an increase of the turbulent intensities when going towards the blade surface.

5. PUBLICATIONS AND PRESENTATIONS

The following papers were published during this period:

1. Lakshminarayana, B., C. Hah, and T. R. Govindan, "Three Dimensional Turbulent Boundary Layer Development on a Fan Rotor Blade," AIAA Paper 82-1007, 1982.
2. Pouagare, M., K. N. S. Murthy, and B. Lakshminarayana, "Three Dimensional Flow Field Inside the Passage of a Low Speed Axial Flow Compressor Rotor," AIAA Paper 82-1006, 1982.

The following presentations were made during the reporting period.

1. B. Lakshminarayana, "Experimental Study of the Rotor Blade Boundary Layer in a Single Stage Fan," IUTAM Symposium on Three Dimensional Turbulent Boundary Layers, Technische Universitat Berlin, Germany, March 29, 1982.
2. B. Lakshminarayana, "Three Dimensional Turbulent Boundary Layer Development on a Fan Rotor Blade," AIAA/ASME Third Joint Thermophysics, Fluids, Plasma and Heat Transfer Conference, St. Louis, Missouri, June 11, 1982.
3. M. Pouagare, "Three Dimensional Flow Field Inside the Passage of a Low Speed Axial Flow Compressor Rotor," AIAA/ASME Third Joint Thermophysics, Fluids, Plasma and Heat Transfer Conference, St. Louis, Missouri, June 11, 1982.

REFERENCES

1. Pouagare, M., J. M. Galmes, B. Lakshminarayana, and K. N. S. Murthy, "Three Dimensional Flow Field Inside Compressor Rotor, Including Blade Boundary Layer," PSU/Turbo 82-1, Progress Report on NASA Grant NSG 3266, January 1982.

2. Chou, P. Y., "On Velocity Correlations and the Solutions of the Equations of Turbulent Fluctuation," Quarterly of Applied Mathematics, Vol. 3, No. 38, 1945.

3. Launder, B. E., G. J. Reece, and W. Rodi, "Progress in the Development of a Reynolds Stress Turbulence Closure," Journal of Fluid Mechanics, Vol. 68, Pt. 3, 1975.

4. Donaldson, C. duP., "A Progress Report on an Attempt to Construct an Invariant Model of Turbulent Shear Flows," Proc. AGARD Conference on Turbulent Shear Flows, London, 1971.

5. Lumley, J. L., "A Model for Computation of Stratified Turbulent Flows," International Symposium on Stratified Flow, Novisibirsk, 1972.

6. Daly, B. J. and F. M. Harlow, "Transport Equations of Turbulence," Physics of Fluids, Vol. 13, p. 2634, 1970.

7. Reynolds, W. C., "Computation of Turbulent Flows--State-of-the-Art, 1970," Stanford University, Mechanical Engineering Department Report MD-27, 1970.

8. Townsend, A. A., "The Uniform Distortion of Homogeneous Turbulence," Quarterly Journal Mech. Appl. Math., Vol. 7, p. 404, 1954.

9. Crow, S. C., "Viscoelastic Properties of Fine-Grained Incompressible Turbulence," Journal of Fluid Mechanics, Vol. 41, p. 81, 1968.

10. Rotta, J. C., "Statistische Theorie Nchthomogener Turbulenz," Z. Phys., Vol. 129, p. 547, 1951.

11. Lumley, J. L., "Second Order Modelling of Turbulent Flows," VKI Lecture Series, Von Karman Institute for Fluid Dynamics, Rhode St. Genese, Belgium, 1979.

12. Aris, R., Vectors, Tensors, and the Basic Equations of Fluid Mechanics, Prentice-Hall, Inc., 1962.

13. Cousteix, J. and B. Aupoix, "Modelisation des Equations aux Tensions de Reynolds dans un Repere en Rotation," La Recherche Aerospatial, No. 4, pp. 275-285, 1981.

14. Bradshaw, P., "The Strategy of Calculation Methods for Complex Turbulent Flows," Imperial College Aerospace Report No. 73-05, 1973.

15. Raj, R., "Pressure Gradient-Velocity Correlations for Flows with Two- and Three-Dimensional Turbulence," Physics of Fluids, Vol. 20, No. 12, 1977.

16. Uberoi, M. S., "Equipartition of Energy and Local Isotropy in Turbulent Flows," Journal of Applied Physics, Vol. 28, p. 1165, 1957.

17. Hanjalic, K. and B. E. Launder, "Contribution Towards a Reynolds-Stress Closure for Low Reynolds Number Turbulence," Journal of Fluid Mechanics, Vol. 74, Pt. 4, pp. 593-610, 1975.

18. Patankar, S. V. and D. B. Spalding, Heat and Mass Transfer in Boundary Layers, A General Calculation Procedure, Intertext Book, London, 1970.

19. Rodi, W., "A New Algebraic Relation for Calculating the Reynolds Stresses," Z. Angew. Math. Mech., Vol. 56, pp. 219-221, 1976.

20. Lohman, R. P., "The Response of a Developed Turbulent Boundary Layer to Local Transverse Surface Motion," Journal of Fluids Engineering, pp. 354-363, September 1976.

21. Koosilin, M. L. and F. C. Lockwood, "The Prediction of Axisymmetric Turbulent Swirling Boundary Layers," AIAA Journal, Vol. 12, No. 4, 1974.

22. Cousteix, J. and B. Aupoix, "Comparison of Various Calculation Methods for Three Dimensional Turbulent Boundary Layer," Second Symposium on Turbulent Shear Flows, The Pennsylvania State University, 1979.

23. Govindan, T. R., B. Lakshminarayana, A. Pandya, and M. Pouagare, "Endwall Flows in Rotors and Stators of a Single Stage Compressor," Progress Report to NASA, PSU/Turbo R81-7, August 1981.

24. Lakshminarayana, B., C. Hah, and T. R. Govindan, "Three Dimensional Turbulent Boundary Layer Development on a Fan Rotor Blade," AIAA Paper 82-1007, 1982.

25. Arzoumanian, E., M. Leborgne, and L. Fulachier, "Turbulent Field of a Boundary Layer Very Close to Axially Rotated Cylinder," Third Symposium on Turbulent Shear Flows, University of California, Davis, September 9-11, 1981.

APPENDIX A

Derivation of $\phi^{\ell}_{k,2}$

$$\phi^{\ell}_{k,2} = \frac{1}{2\pi} \iiint_{vol} U^{*m}_{1,r_1} \overline{u'^{r}_{,m} u'^{\ell}_{,k}} \frac{dV'_1}{||\vec{\xi}||} = \frac{1}{2\pi} \iiint_{vol} U^{**}_{1,r_1} \left(\overline{u'_1{}^{r} u'^{\ell}}\right)_{,m_1 k} \frac{dV'_1}{||\vec{\xi}||} \tag{A-1}$$

because the derivation at point x and x_1 are independent. It is straightforward in the case of cartesian coordinates. In the case of generalized tensor see Aris [12]. Let us define new independent variables as follows:

$$\vec{x} = \vec{X} \quad \text{and} \quad \vec{\xi} = \vec{x}_1 - \vec{x}$$

with $\vec{x} = x^{\ell}$ and $\vec{x}_1 = x^{\ell}_1$; $\vec{\xi} = \xi^{\ell}$

then $U^{*m}_{1,r_1} = \frac{\partial x^m_1}{\partial \xi^{m'}} \frac{\partial \xi^{r''}}{\partial x^{r}_1} U^{*m''}_{,r''} = U^{*m''}_{,r''}$

and

$$\left(\overline{u'_1{}^{r} u'^{\ell}}\right)_{,m_1 k} = \frac{\partial x^{r}_1}{\partial \xi^{r''}} \frac{\partial x^{\ell}}{\partial x^{\ell''}} \frac{\partial \xi^{m''}}{\partial x^{m}_1} \frac{\partial x^{k''}}{\partial x^{k}} \left(\overline{u'^{r''} u'^{\ell''}}\right)_{,k''m''} = \left(\overline{u'^{r''} u'^{\ell''}}\right)_{,k''m''} = \left(\overline{u'^{r''} u'^{\ell}}\right)_{,k''m}$$

Then with the hypothesis of homogeneous flow the $U^{*m''}_{,r''}$ is independent of the point (1), therefore it can be shown [3,10,14]

$$\phi^{\ell}_{k,2} = \frac{U^{*m''}_{,r''}}{2\pi} \iiint_{vol} \left(\overline{u'^{r''} u'^{\ell}}\right)_{,k''m} \frac{dV'_1}{||\vec{\xi}||} = U^{*m''}_{,r''} a^{r''\ell}_{m''k} \tag{A-2}$$

as the indices m' and r' are dummy se can rewrite equation A-2 as follows:

$$\phi^{\ell}_{k,2} = U^{*m}_{,r} a^{r\ell}_{mk} \tag{A-3}$$

APPENDIX B

Patankar-Spalding Numerical Method for Two-Dimensional Boundary Layers

1. Introduction

We are going to give some indications on the numerical method established by Patankar and Spalding in 1967 and modified in 1970 by these authors. The presentation will be brief and for further information the reader may want to refer to the book entitled HEAT AND MASS TRANSFER IN BOUNDARY LAYERS--A GENERAL CALCULATION PROCEDURE, by S. V. Patankar and D. B. Spalding, Intertextbook, London, 1970. The method is of the marching type and is adapted for two-dimensional boundary layers. The boundary layers approximations lead to a system of parabolic, partial derivatives equations. With the Patankar-Spalding method we may calculate a purely dynamic boundary layer, as well as a thermal boundary layer, or whatever contaminant evolution.

This method does not need any boundary layer similitude hypothesis, and the principal characteristics of the method are the following:

-- A non-dimensional streamfunction is used as independent variable, then the couple (x,y) of the physical plane is replaced by the couple (x,w) which allows an automatic adaptation of the thickness at each abscissa x.

-- The implicit scheme of discretization using the micro-integral technique, verifies the conservative properties of the partial derivatives equations and is unconditionally stable.

-- The marching solution is very well adapted to calculate a flow, very quickly and using a really few memory storage in the computer.

-- To invert the matrices, the method uses a tridiagonal algorithm derived from the Gauss method, this is done with very simple iterative formulas.

2. Formulation of the Equation

Here, we will use a two-dimensional cartesian frame to present the derivation of the equations.

For each transport quantity ϕ of interest in the boundary layer, its equation can take the form:

$$\rho\, U \frac{\partial \phi}{\partial x} + \rho\, V \frac{\partial \phi}{\partial y} = \frac{\partial \Gamma_{eff}\ \partial \phi / \partial y}{\partial y} + S_\phi \qquad (1)$$

where Γ_{eff} is an effective diffusivity coefficient and S_ϕ represents a "source" term.

The continuity equation is joined to equation (1).

Using Von Mises transformation, where (x,y) is replaced by (x,ψ), ψ is the streamfunction ($\rho\, U = \partial\psi/\partial y$), equation (1) becomes:

$$\frac{\partial \phi}{\partial x} = \frac{\partial \rho\, U\, \Gamma_{eff}\ \partial \phi / \partial \psi}{\partial \psi} + \frac{S_\phi}{\rho U} \qquad (2)$$

In this new coordinate system (x,ψ), the grid is automatically adapting to the growth of the boundary layer thickness. However, for simplicity in the definition of boundary conditions, it is useful to introduce another coordinate system (x,w) where w is defined by $w = \psi - \psi_I / \psi_E - \psi_I$ and ψ_E, ψ_I are respectively the values of ψ at each boundary. We have then:

$$w_I = 0 \quad , \quad w_E = 1$$

$$\frac{d\psi_I}{dx} = -\rho_I V_I \quad , \quad \frac{d\psi_E}{dx} = -\rho_E V_E$$

In this new coordinate system, equation (1) becomes:

$$\underset{\text{conv.}}{\frac{\partial \phi}{\partial x} + (a + bw) \frac{\partial \phi}{\partial w}} = \underset{\text{dif.}}{\frac{\partial c\ \partial \phi / \partial w}{\partial w}} + \underset{\text{source}}{d_\phi} \qquad (3)$$

where a and b are functions of x

$$a = \frac{\rho_I V_I}{\psi_E - \psi_I} \quad ; \quad b = \frac{\rho_E V_E - \rho_I V_I}{\psi_E - \psi_I}$$

where c and d_ϕ are functions of x, w, ϕ

$$c = \frac{\rho U \Gamma_{eff}}{(\psi_E - \psi_I)^2} \quad ; \quad d_\phi \text{ depends on the definition of the quantity } \phi \text{ (for example for velocity U, } d_\phi \text{ is the pressure gradient)}$$

The mass transfer rates $m'' = \rho V$ through the boundaries I and E are specified by the nature of the boundaries (symmetry axis, wall, free boundary, ...). In the case of a symmetry axis or a wall, these rates are zero. For a free boundary G, Patankar and Spalding express the mass transfer rate as a function of the effective diffusion, as follows:

$$m''_G = \lim_{y \to y_G} \left[\frac{\partial / \partial y \ (\mu_{eff} \ \partial U / \partial y)}{\partial U / \partial y} \right]$$

This necessitates the knowledge of the effective viscosity. We may note that it is this transfer rate which controls the "entrainment" of the marching solution, then it is important to control the definition of this mass transfer rate m''_G. Some damping functions may be used to diminish the exchange of flow through the boundary G when that is necessary (see Patankar-Spalding).

Now, equation (3) is a non-linear partial derivatives equation with boundary conditions depending on the specificity of the physical problem. Then, to solve this equation, in the general case, we have to use a finite difference technique which is described hereafter.

3. Numerical Discretization

Equation (3) is discretized and integrated by a marching method in direction x. At each step of the integration, the values of ϕ are known at each point of the grid in direction w for a given section, and we may get the values of ϕ for the next section.

Generally, to obtain a finite difference form of a partial derivative equation we may use the Taylor series. But it is also possible to obtain the finite difference equation considering each term of the non-discretized equation as an average integration on a small volume around each point of discretization; this volume is called the control volume. This is the process which is used by Patankar-Spalding, introducing certain hypotheses relatively to the nature and the variation of ϕ between grid nods. Two assumptions are made on the variation of ϕ. First it is supposed, that ϕ varies linearly between nodes w_i, and secondly, ϕ is set constant in the interval $]x_U, x_D]$ and equal to its value in x_D. Then, for the non-boundary zone, equation (3) may be integrated in the rectangular dot domain presented below (Figure 1) as follows:

$$\left[\int_{-}^{+} \phi_D dw - \int_{-}^{+} \phi_U dw\right]/\delta x + \left[\{(a + bw)\phi_D\}_+ - \{(a + bw)\phi_D\}_-\right] - b \int_{-}^{+} \phi_D dw = \left[\left(c \frac{\partial \phi}{\partial w}\right)_+ - \left(c \frac{\partial \phi}{\partial w}\right)_-\right] + \int_{-}^{+} d_\phi dw \qquad (4)$$

Equation (4) can be put, then, in the recurrent form:

$$\phi_{Di} = A_i \phi_{D_{i+1}} + B_i \phi_{D_{i-1}} + C_i \qquad (5)$$

where A_i, B_i, C_i are coefficients and are known at each node.

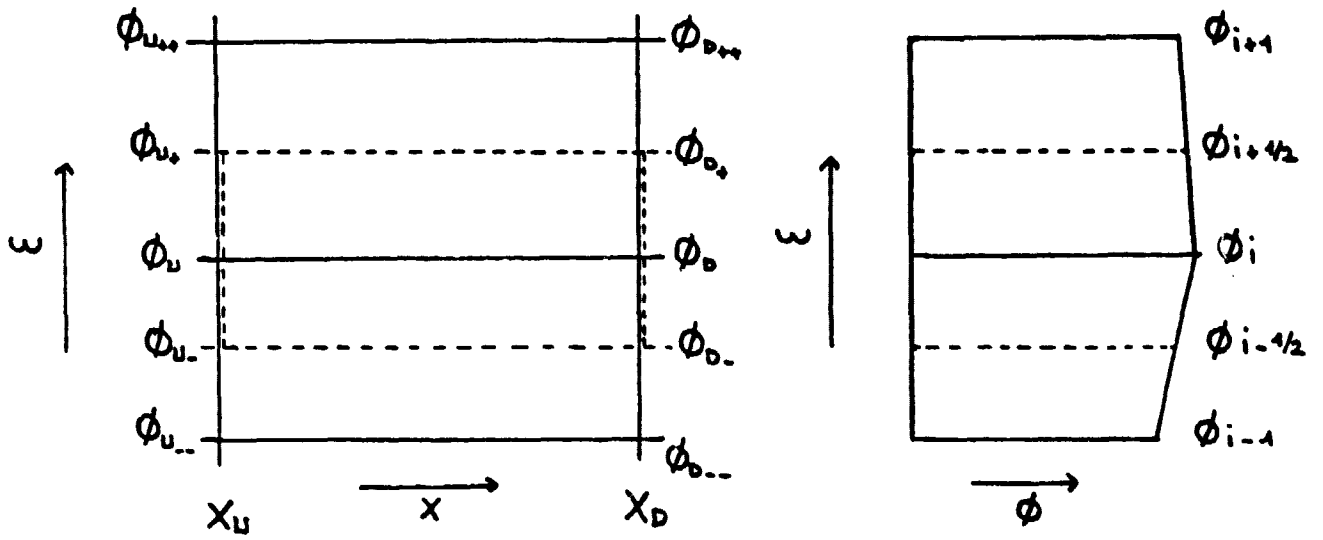

Figure 1.

In the case of the boundary region, a different scheme is used. On boundary I, for example (Fig. 2) a fictitious value ϕ_2, called the "slip value" is introduced such as the linear interpolation of ϕ between nodes w_2 and w_3 gives the right slope at the intermediate point $w_{2.5}$. In fact, the boundary regions are important as they control the fluxes and entrainment rate, the variations of $\phi(w)$ could not be supposed linear in a domain which is only half of an equivalent domain away from the boundaries. The values of ϕ at the boundaries I and E are given by the boundary conditions; if the grid is numbered from 1 to N + 3, we need two discretized equations to relate ϕ_2 and ϕ_{N+2} to, respectively, ϕ_1 and ϕ_3, and ϕ_{N+1} and ϕ_{N+3}. Then we may write:

$$\phi_2 = A_2\phi_3 + B_2\phi_1 + C_2 \quad ; \quad \phi_{N+2} = A_{N+2}\phi_{N+3} + B_{N+2}\phi_{N+1} + C_{N+2}$$

where A_2, B_2, C_2 and A_{N+2}, B_{N+2}, C_{N+2} are known and include the boundary conditions.

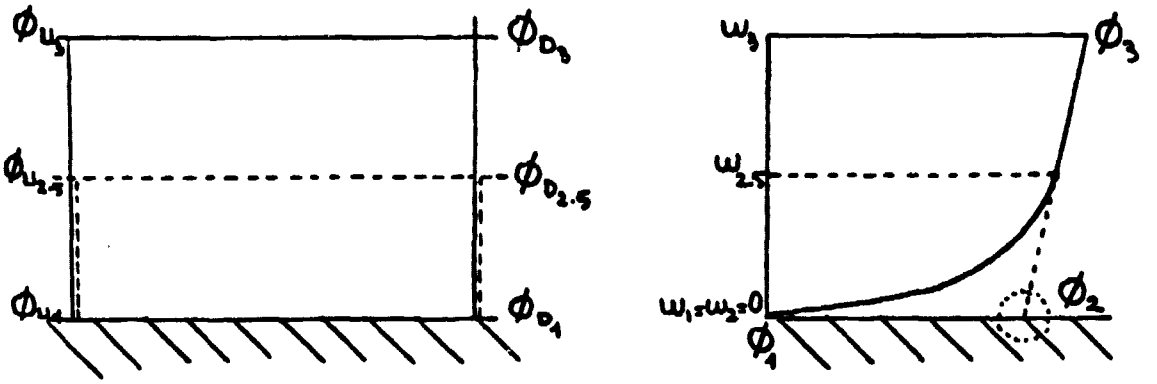

Figure 2.

Then, we obtain the following tridiagonal system:

$$\phi_i = A_i\phi_{i+1} + B_i\phi_{i-1} + C_i \quad (i = 2, \ldots, N+2) \tag{6}$$

The system is solved, using the so-called Thomas algorithm:

$$\phi_i = \alpha_i\phi_{i+1} + \beta_i \quad (i = 2, \ldots, N+2)$$

with

$$\alpha_i = \frac{A_i}{1 - B_i\alpha_{i-1}} \quad ; \quad \beta_i = \frac{B_i\,\beta_{i-1} + C_i}{1 - B_i\alpha_{i-1}}$$

$$(i = 2, \ldots, N+1) \qquad (i = 2, \ldots, N+2)$$

$$\alpha_1 = A_1 \qquad \beta_1 = B_1$$

Then the values $\phi(x,w)$ are known for each w; if we want to locate the value in the physical plane (x,y), we have to compute the y_i at each station x. In the particular case of a plane flow, the value y corresponding to w is given by:

$$y_i = (\psi_E - \psi_I) \int_0^{w_i} \frac{dw}{\rho U}$$

Entrainment Rate

In the case of a wall at the boundary I(E), $m''_I(m''_E)$ is given by the wall conditions (blowing, suction, etc.).

In the case of a free boundary, Patankar and Spalding have proposed the following formulations:

$$\begin{cases} m''_I = 2 \dfrac{\mu_{eff_{2.5}}}{y_3 - y_2} \\ m''_E = 2 \dfrac{\mu_{eff_{N+1.5}}}{y_{N+2} - y_{N+1}} \end{cases}$$

which come from the expression:

$$m''_G = \lim_{y \to y_G} \left[\frac{\partial \mu_{eff}}{\partial y} + \mu_{eff} \frac{\partial^2 U}{\partial y^2} / \frac{\partial U}{\partial y} \right]$$

where the second term is neglected. Then the entrainment rate is always positive, and by the way, instabilities of the kind positive-negative-positive in calculation of the rate are avoided.

Source Terms

Different procedures are applicable to discretize the sources S_ϕ

$$S_\phi = (\psi_E - \psi_I) \int_{i-1/2}^{i+1/2} d_\phi \, dw$$

S_ϕ is linearized in ϕ and is written as:

$$S_\phi = S_U + \phi_D S_D$$

For example, for the U component equation the source term is the pressure gradient, and is given by:

$$\begin{cases} S_U = -\left(\frac{\partial p}{\partial x}\right)_i \frac{y_{i+1} - y_{i-1}}{2} \\ \\ S_D = 0 \end{cases}$$

In the general case, for example, total enthalpy, kinetic energy, dissipation rate, many decompositions are possible.

We may put the positive sources in S_U and the negative ones in S_D, or put the proportional sources to ϕ in S_D, while the others are put in S_U, or also put all the terms in S_U and in S_D divided by ϕ_U(Launder). In fact, it does not seem that a particular technique is better than another one.

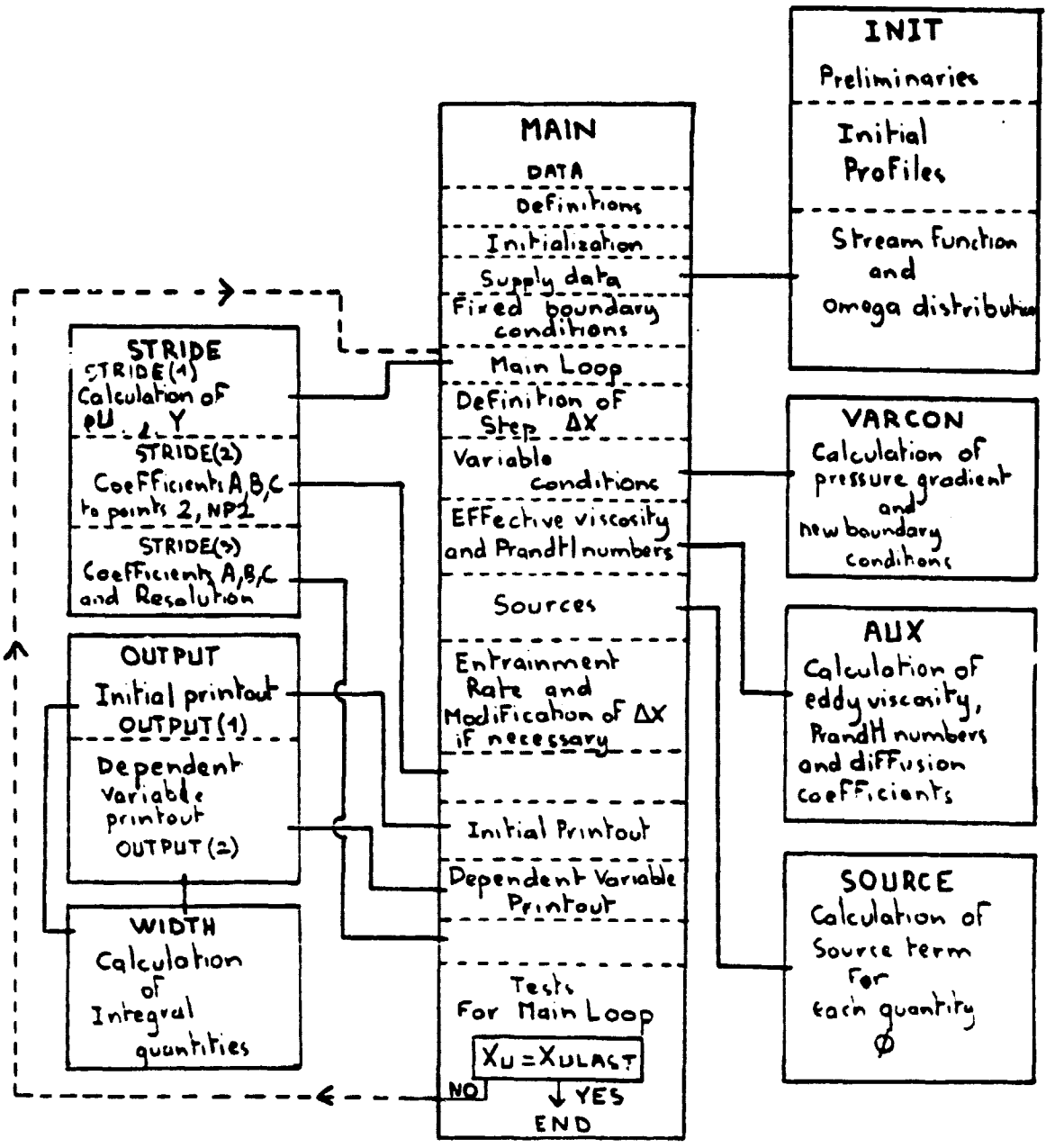

CHART

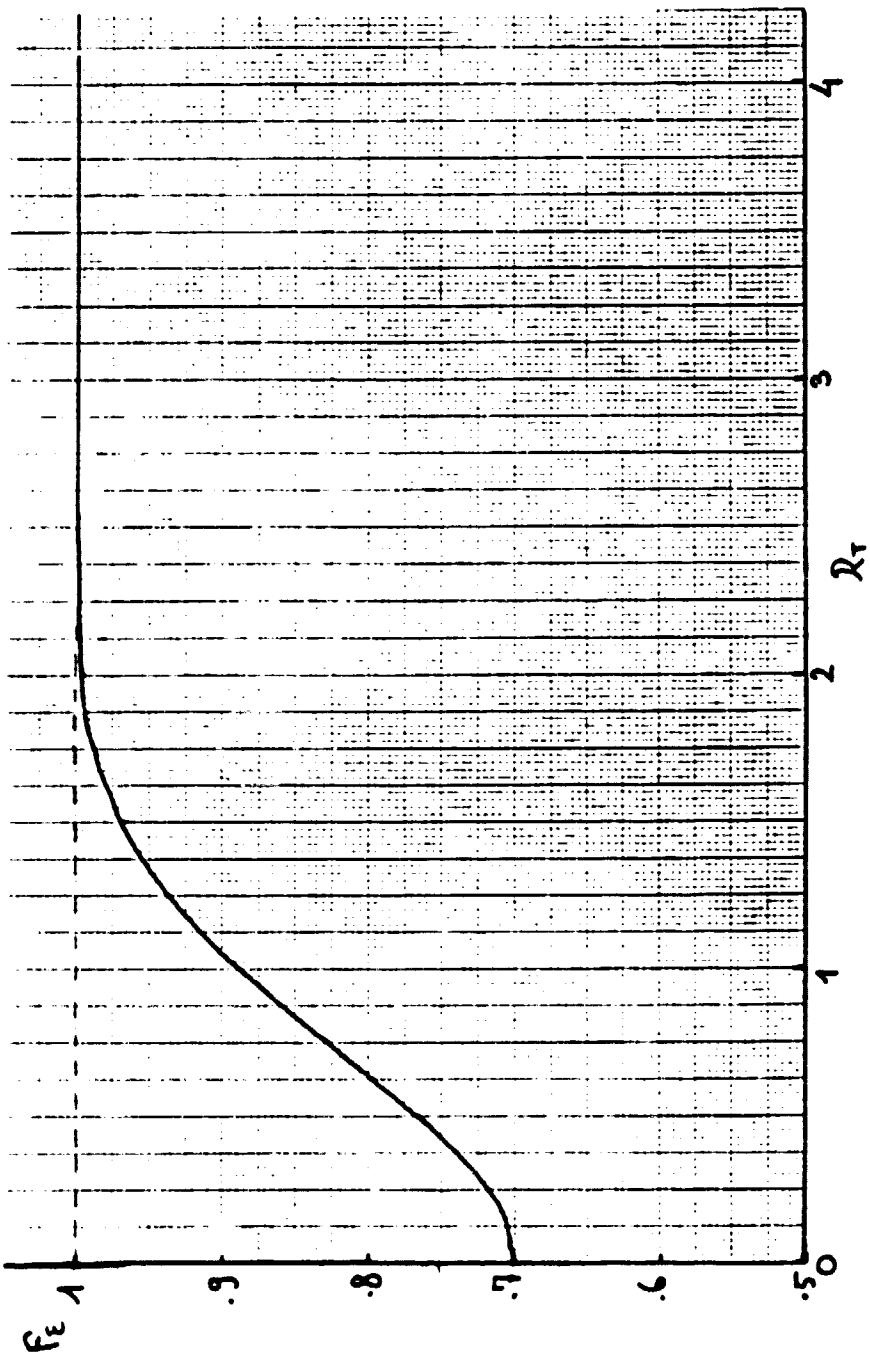

Figure 1. Evolution of correction function F_ϵ in dissipation equation, relative to the local turbulent Reynolds number, R_T

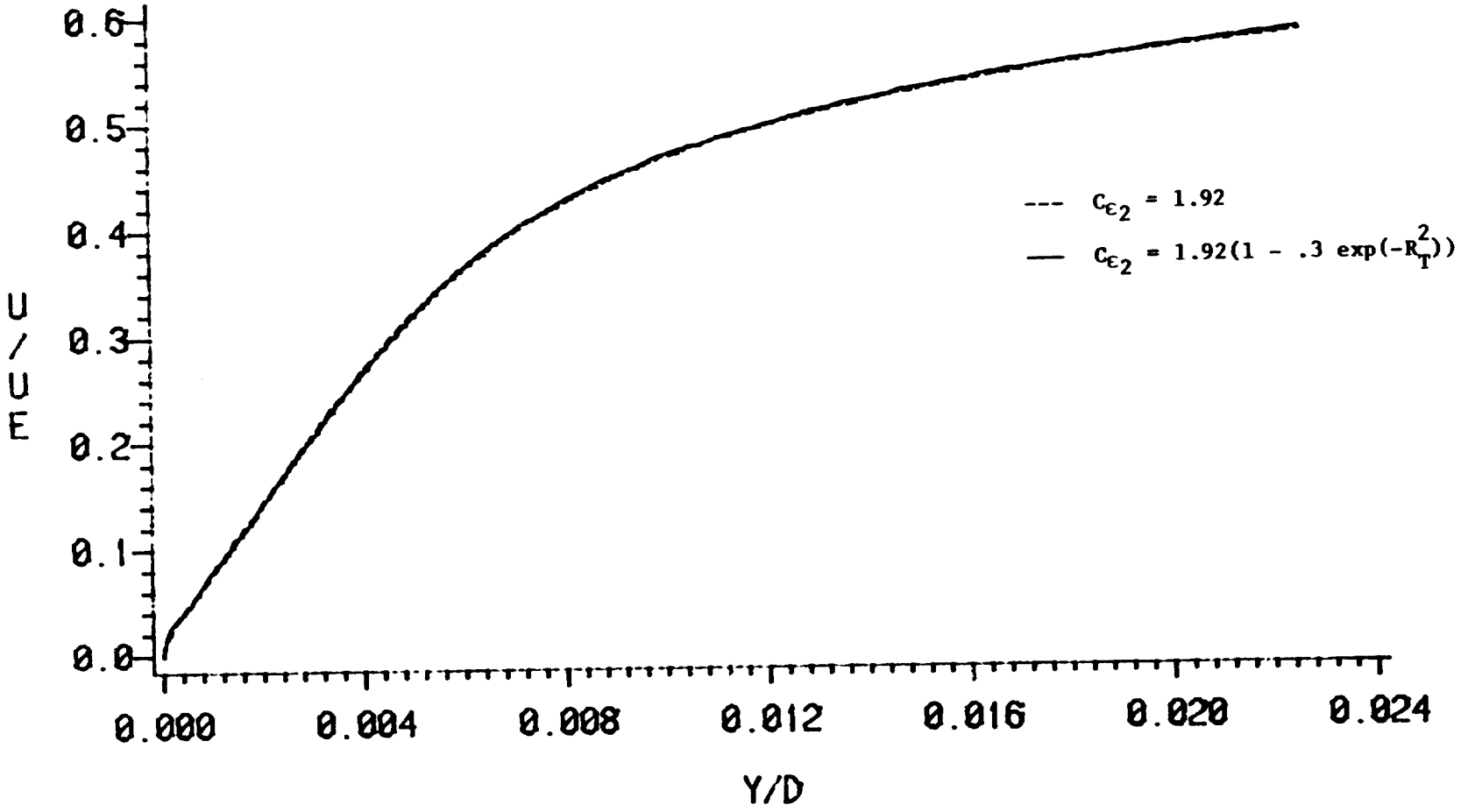

X=40.64 CM

Figure 2. Comparison of calculation with and without function F_ϵ
Velocity profile, U/U_e

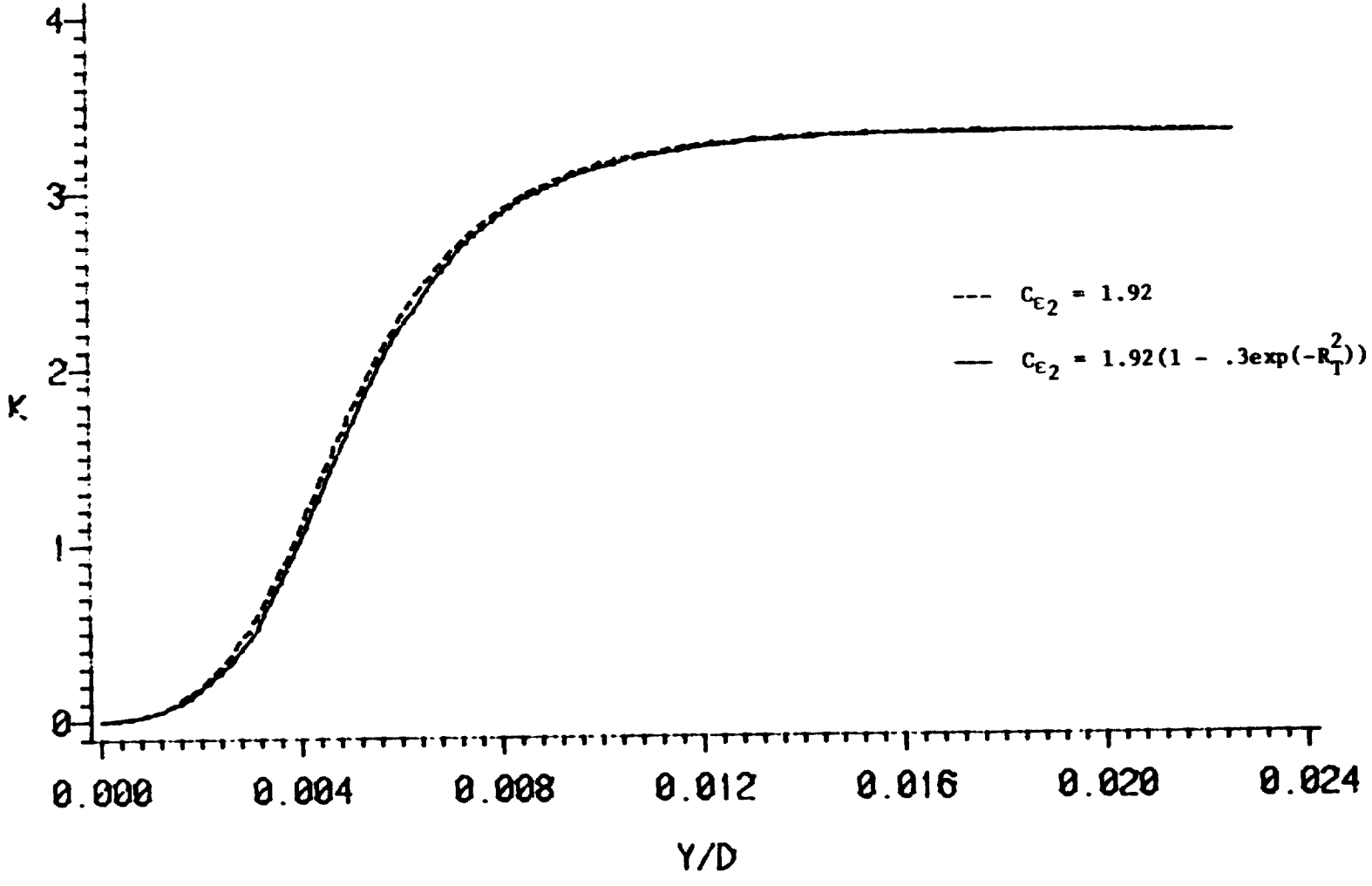

Figure 3. Comparison of calculation with and without function F_ε
Turbulent kinetic energy, k/U_T^2

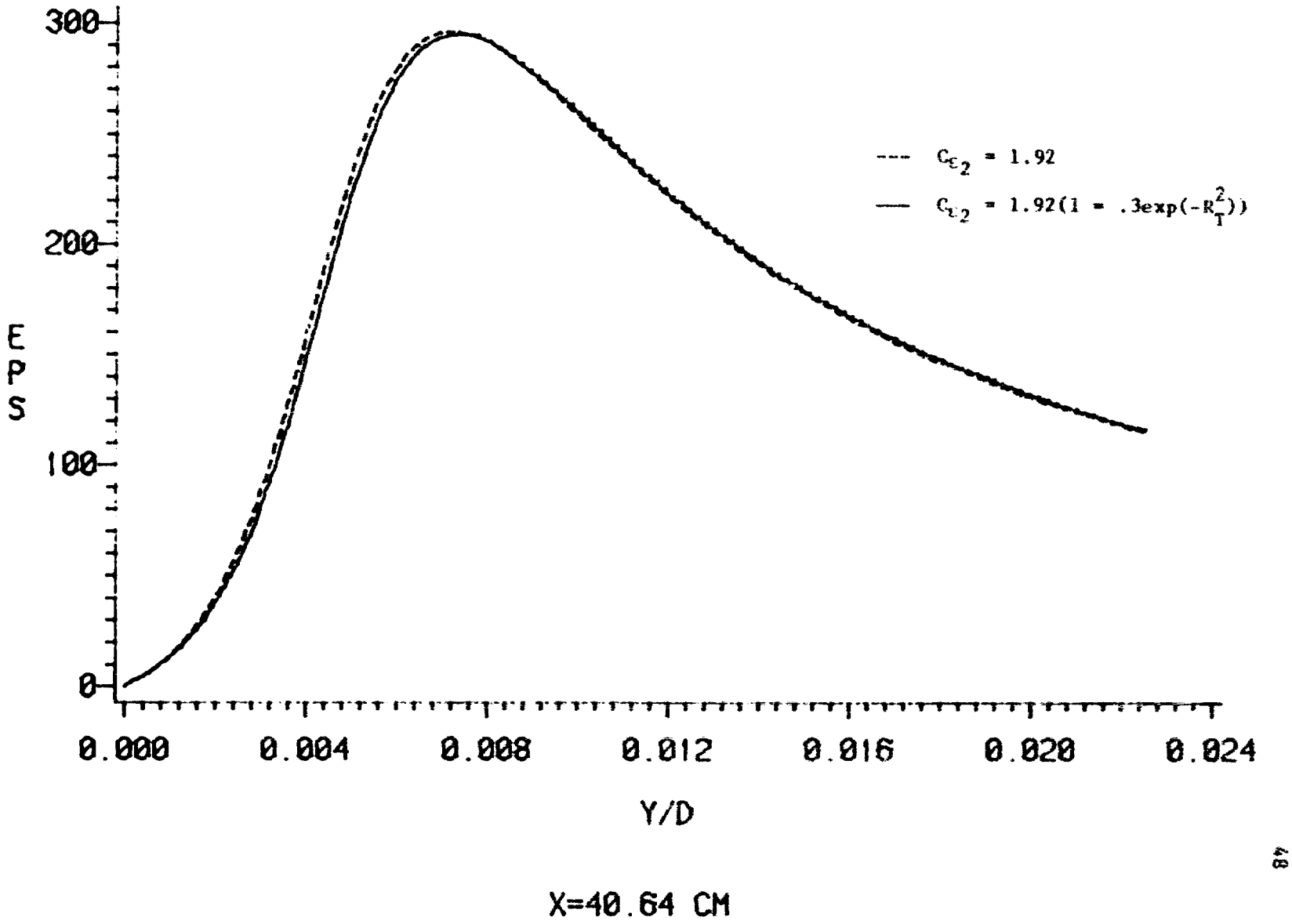

Figure 4. Comparison of calculation with and without function F_ε
Dissipation rate, $\delta\varepsilon/U_\tau^3$

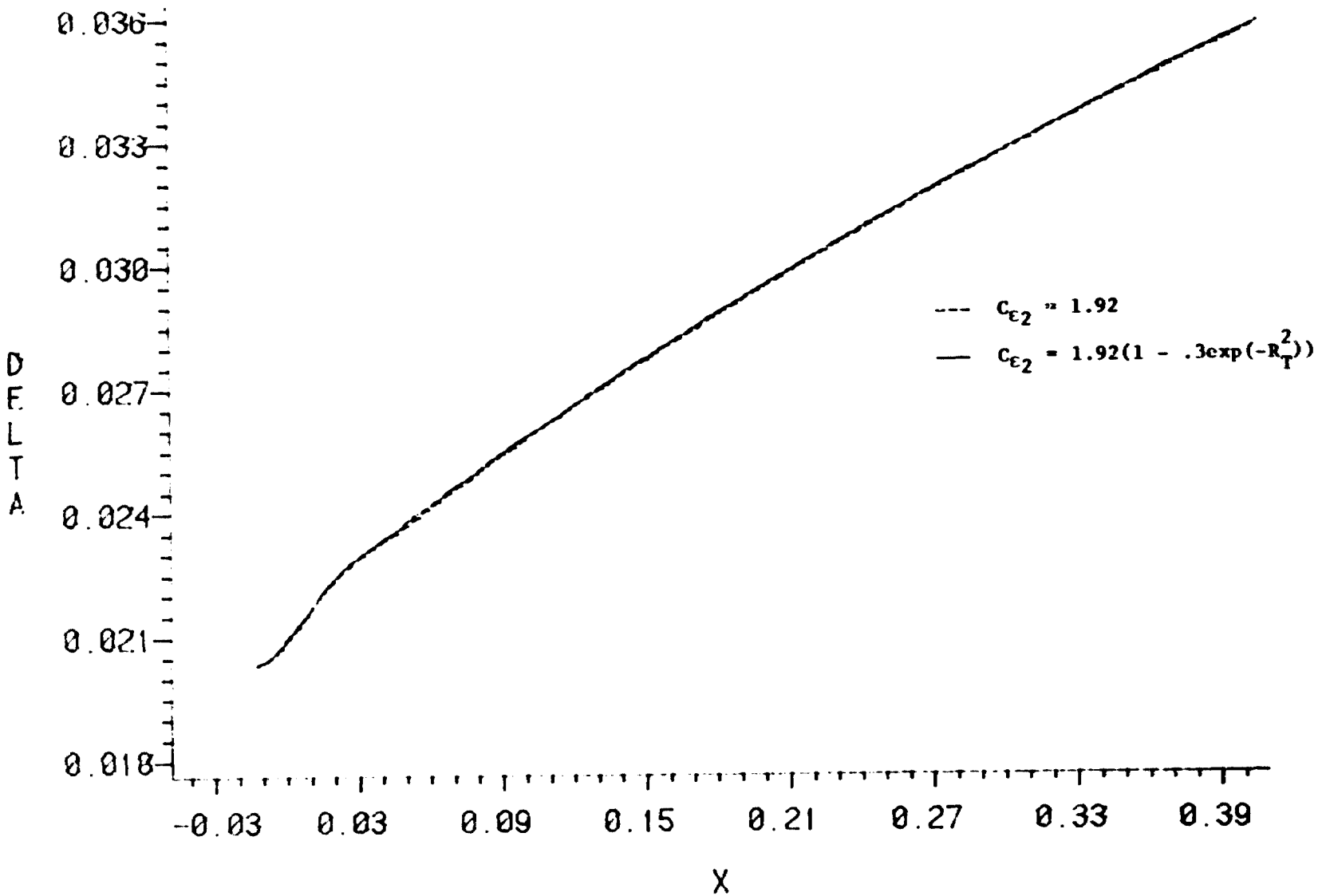

Figure 5. Comparison of calculation with and without function F_ε
Boundary layer thickness (in meter)

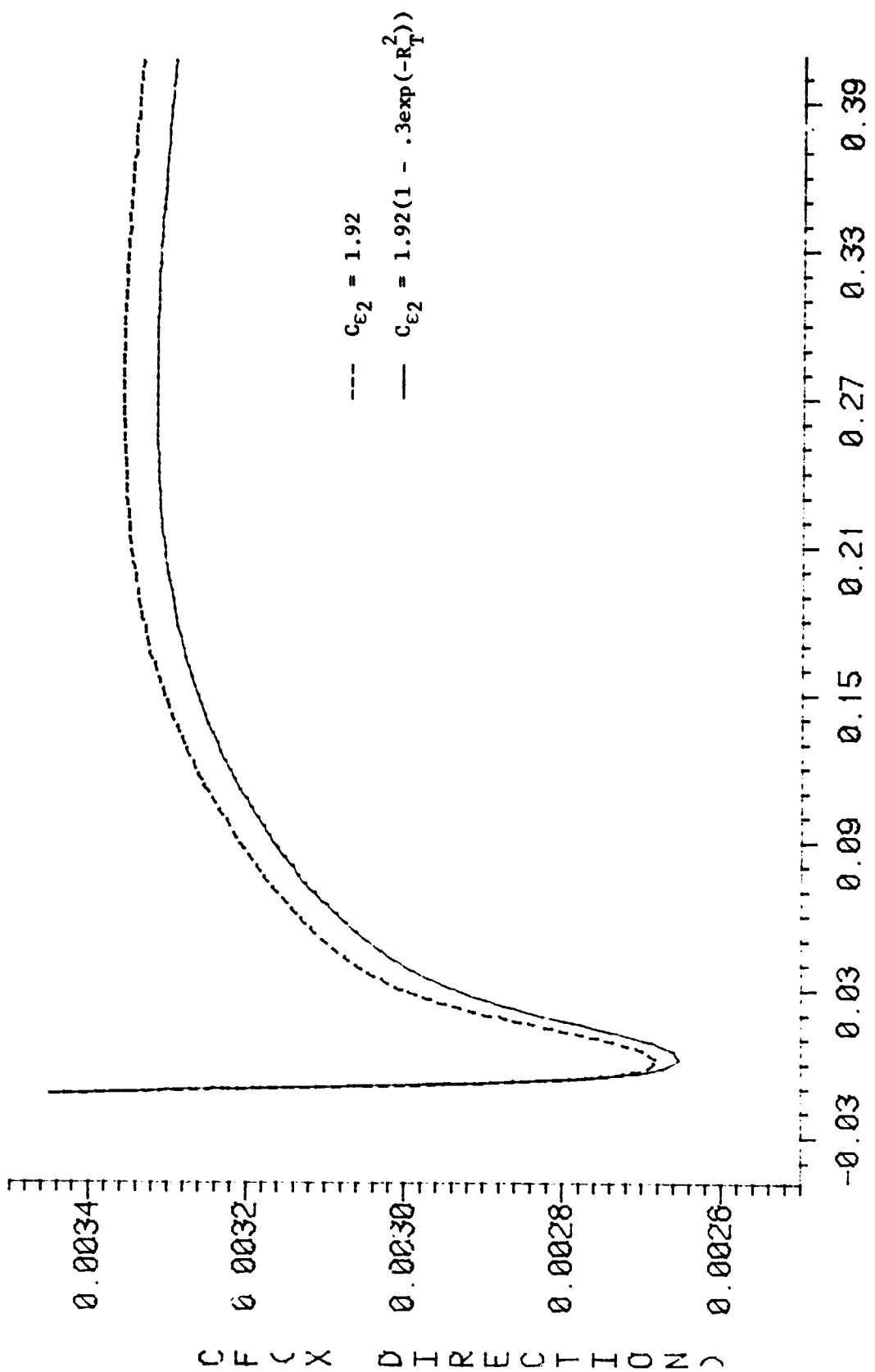

Figure 6. Comparison of calculation with and without function F_ε

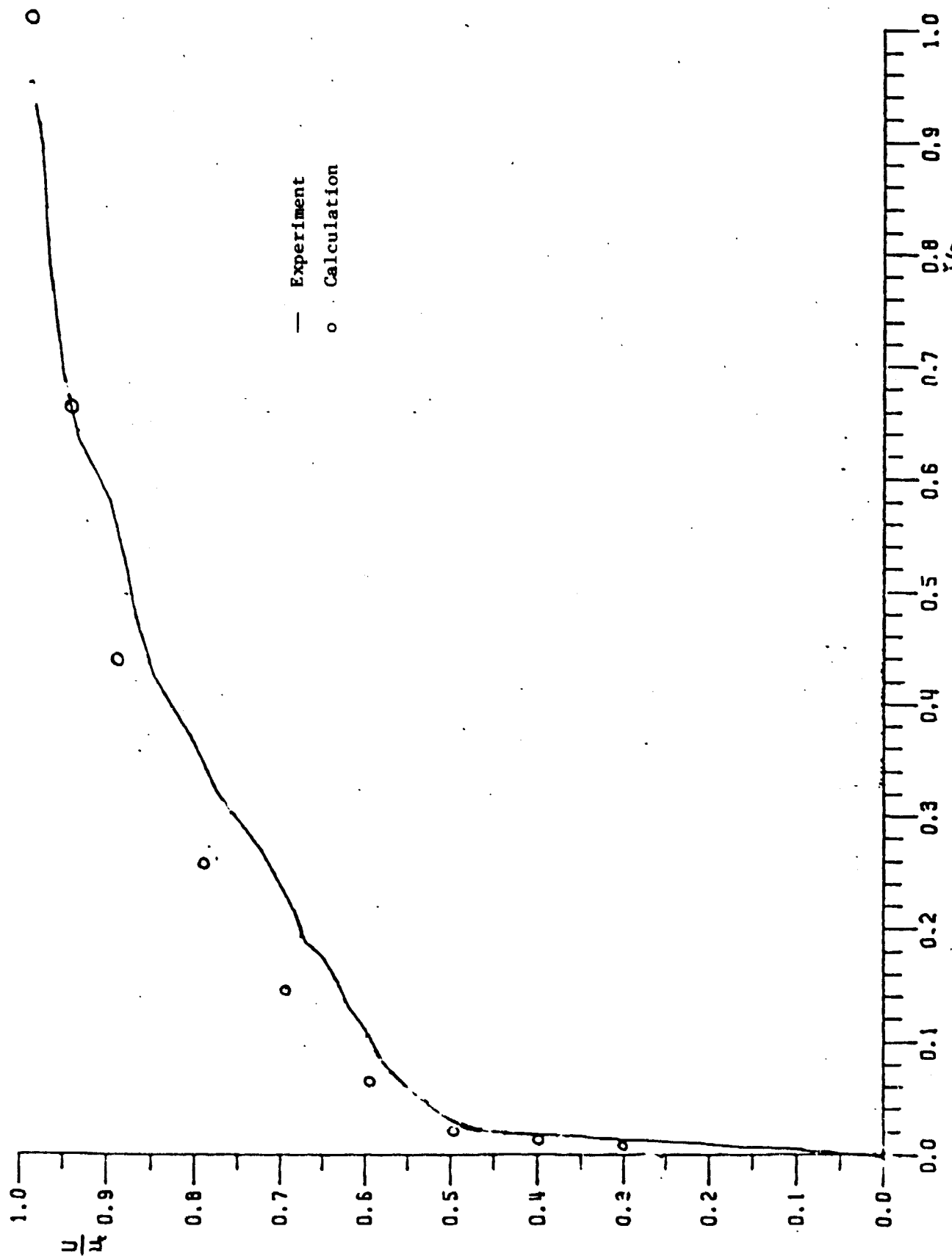

Figure 7. Comparison with Lohman's data; $W_c/U_e = 1.45$ (where W_c is the speed of rotation of the cylinder)
Axial velocity profile

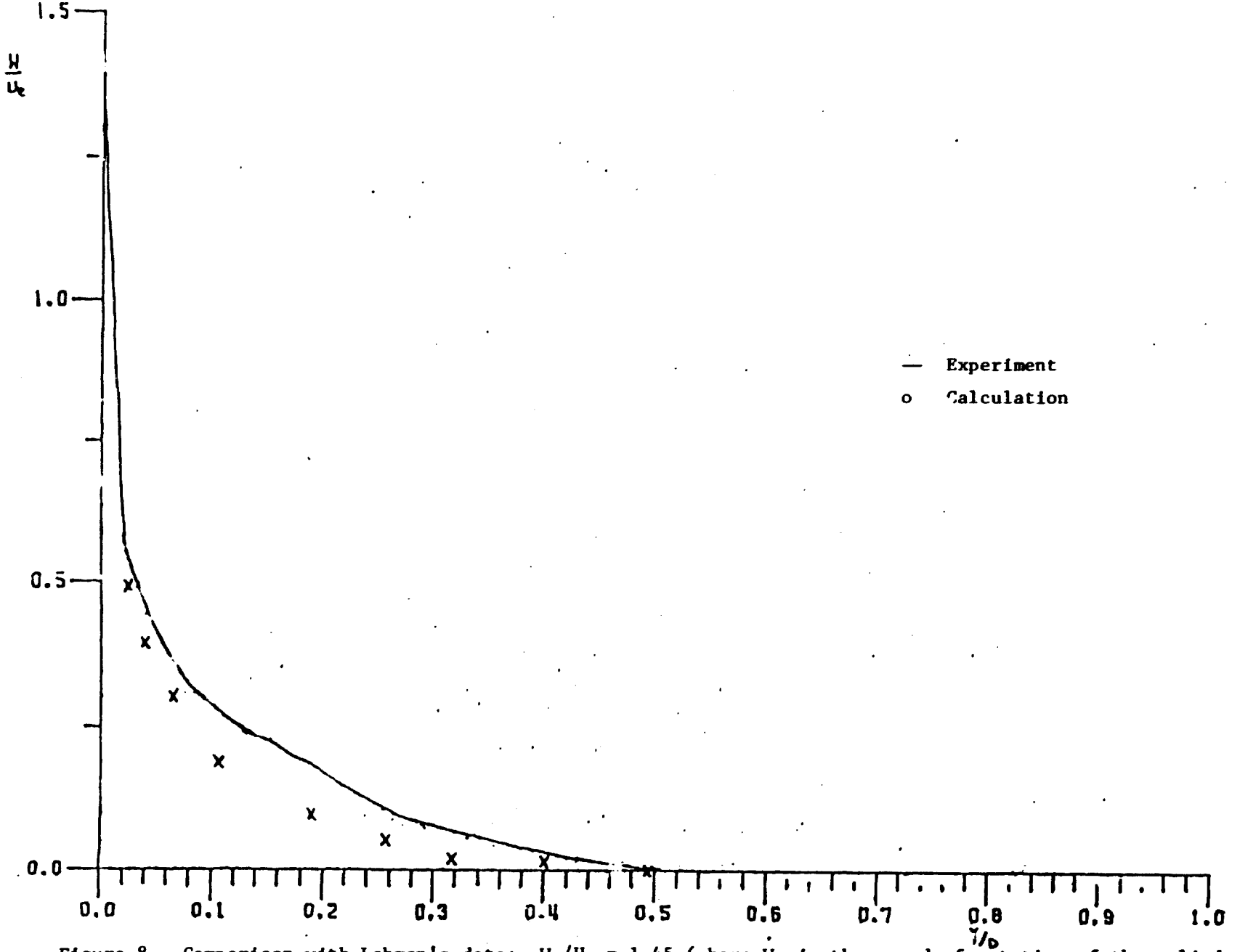

Figure 8. Comparison with Lohman's data; W_c/U_e = 1.45 (where W_c is the speed of rotation of the cylinder) Tangential velocity profile

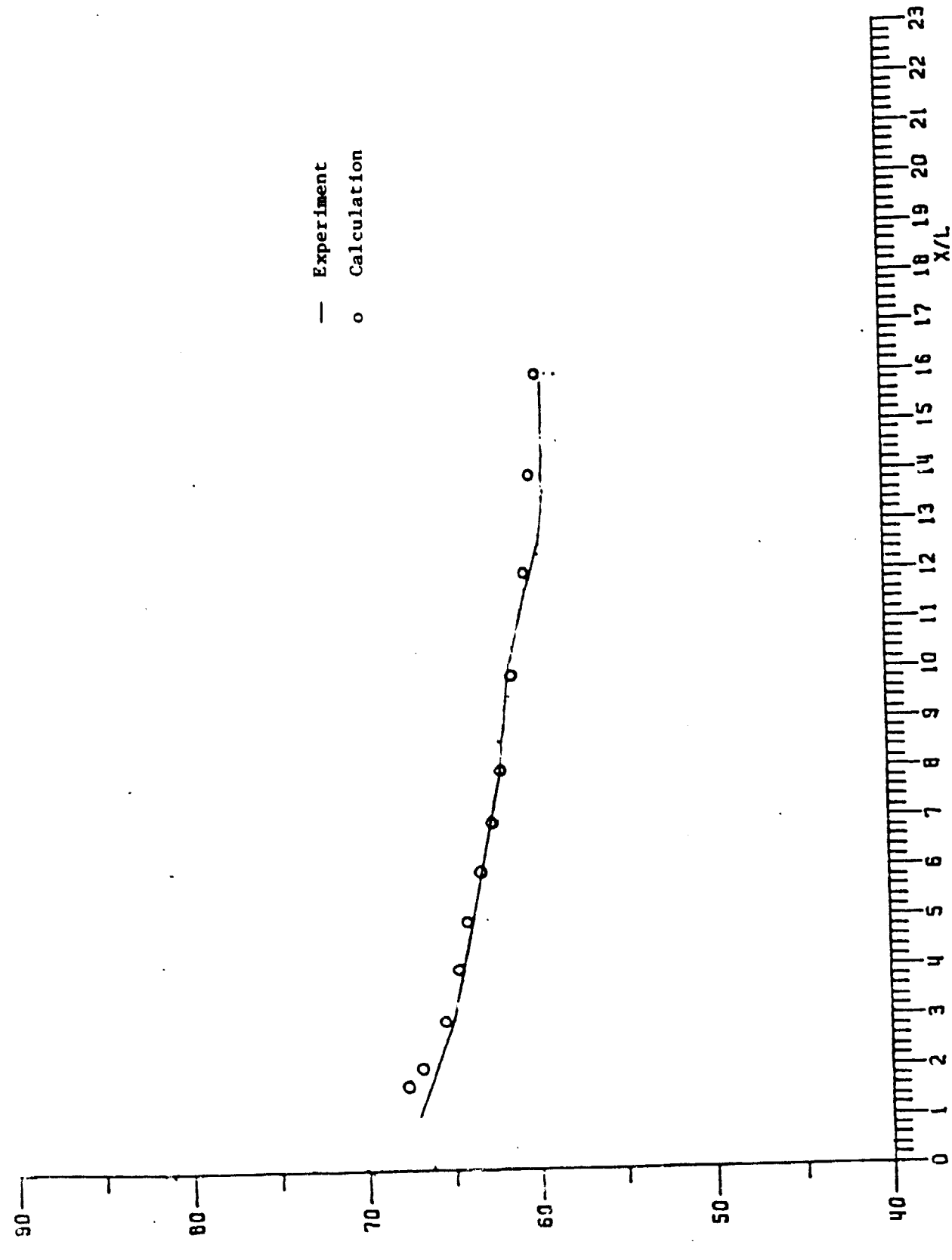

Figure 9. Comparison with Lohman's data; $W_c/U_e = 1.45$ (where W_c is the speed of rotation of the cylinder)
Limiting streamline angle

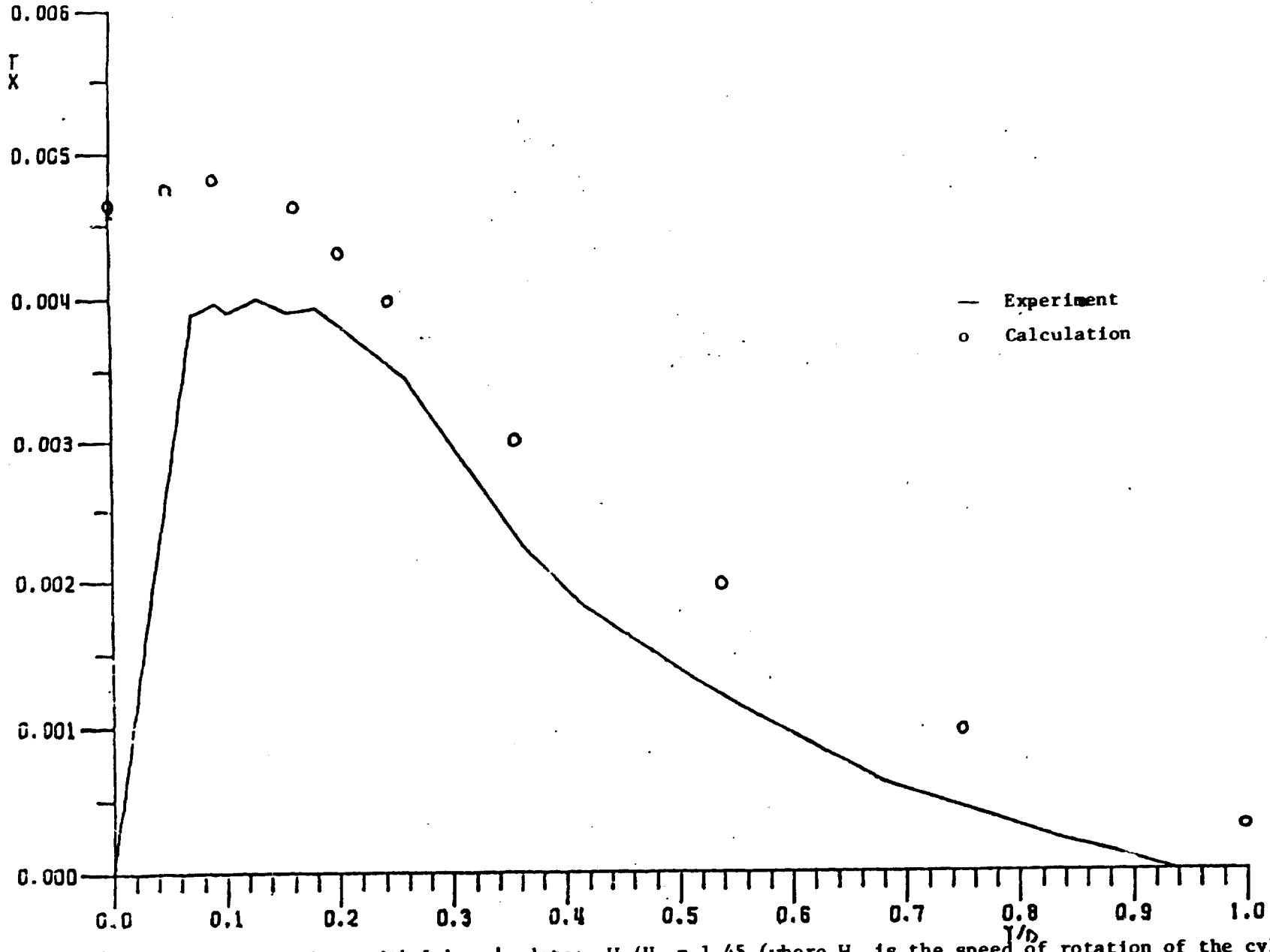

Figure 10. Comparison with Lohman's data; W_c/U_e = 1.45 (where W_c is the speed of rotation of the cylinder) Shear stress in axial direction

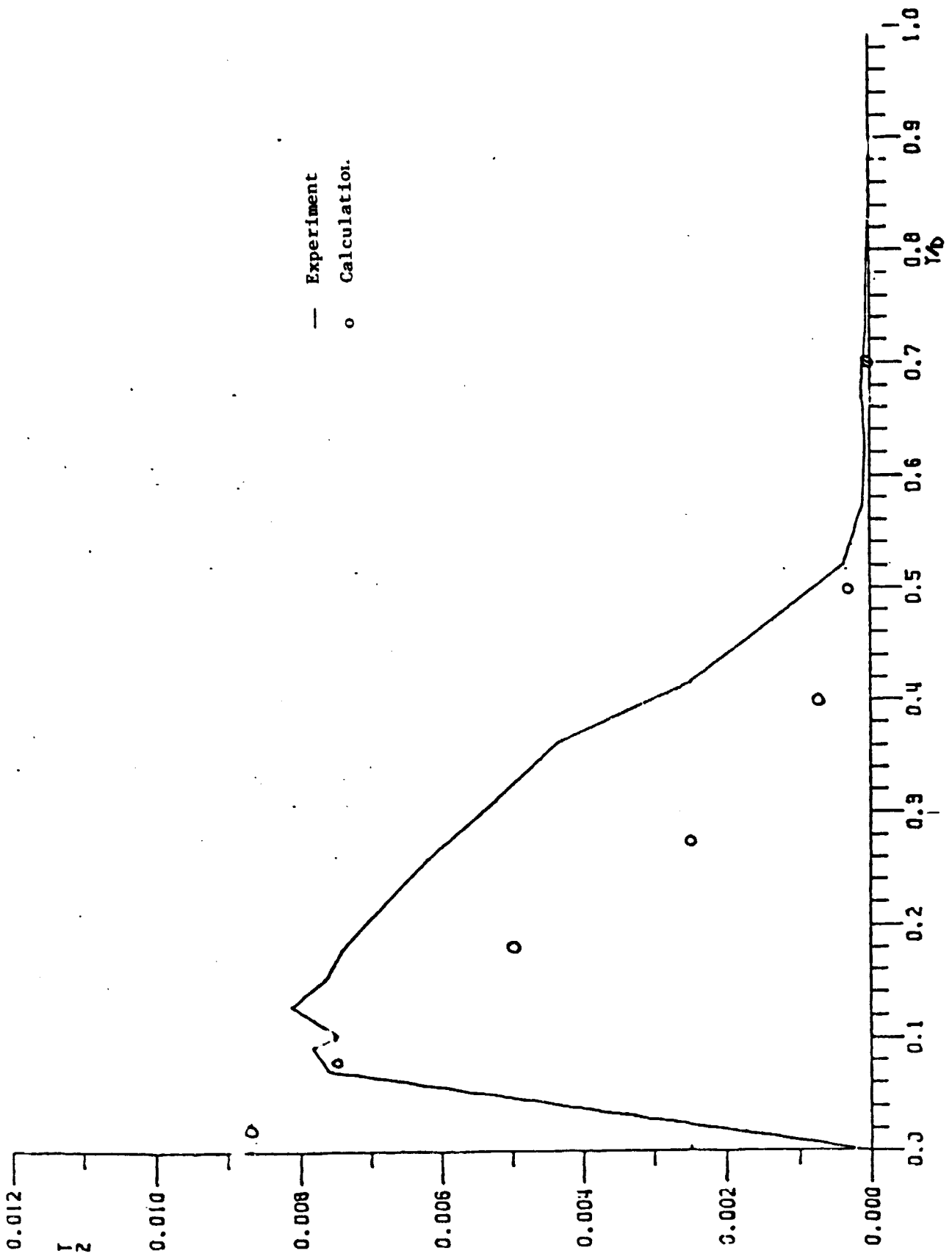

Figure 11. Comparison with Lohman's data; $W_c/U_e = 1.45$ (where W_c is the speed of rotation of the cylinder)
Shear stress in tangential direction

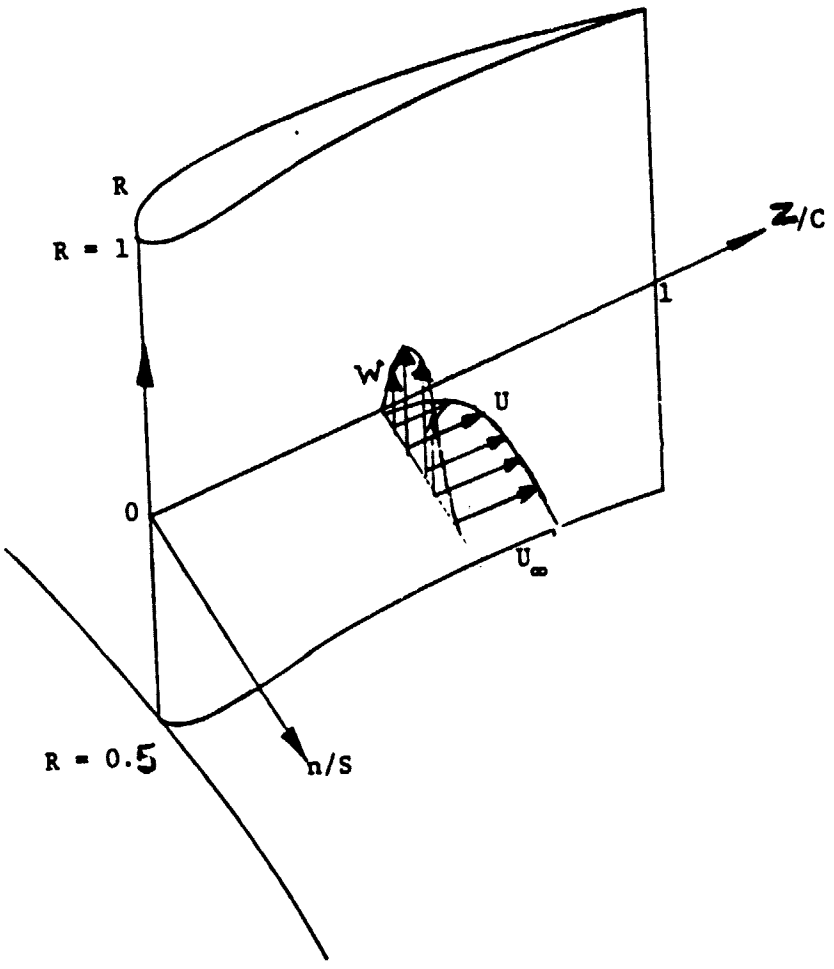

Figure 12. Nature of blade boundary layer and notations used

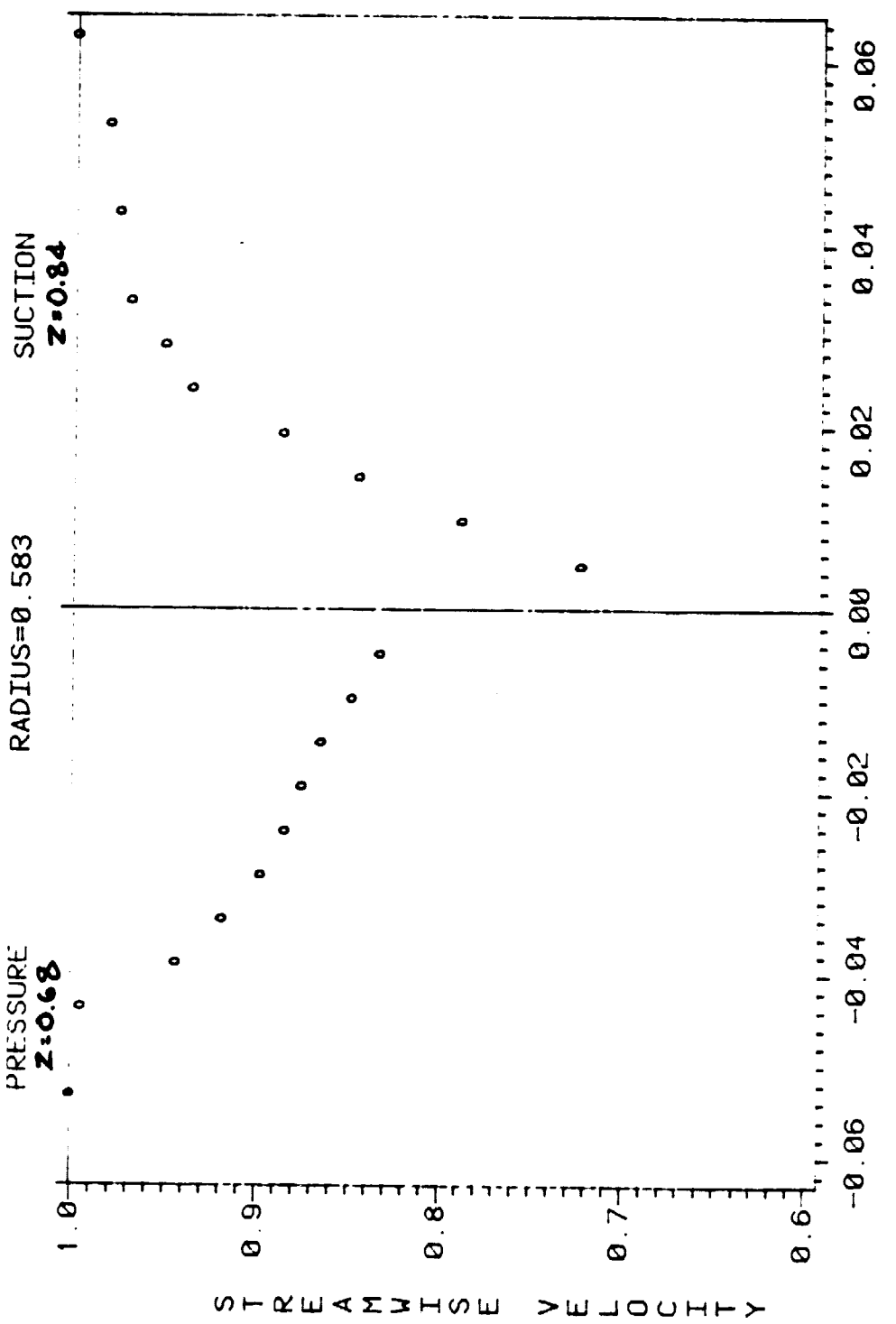

Figure 13. Streamwise velocity (U_s) profiles, R = 0.583, z = 0.68 (P.S.), z = 0.84 (S.S.)

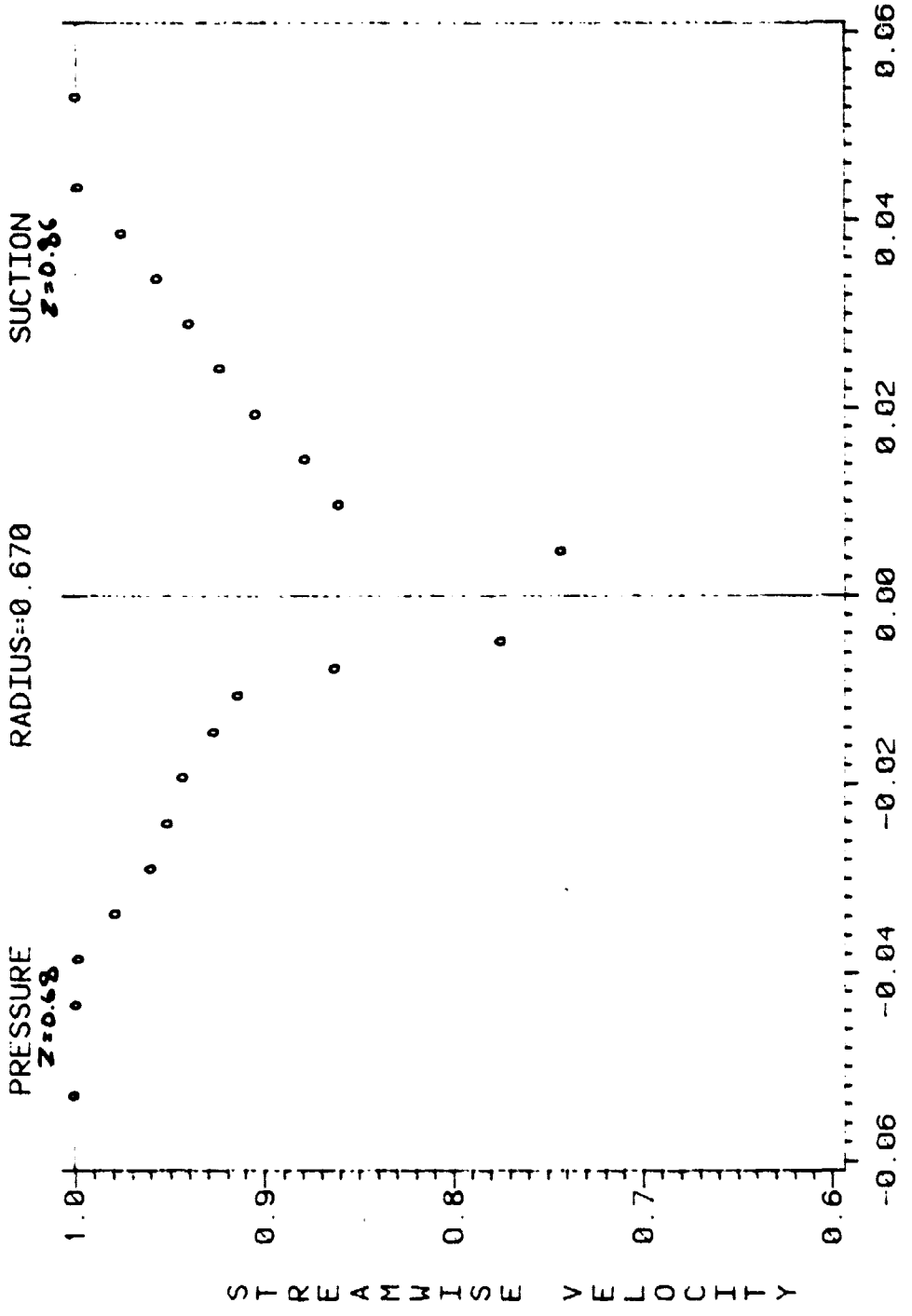

Figure 14. Streamwise velocity (U_s) profiles, R = 0.67, z = 0.68 (P.S.), z = 0.86 (S.S.)

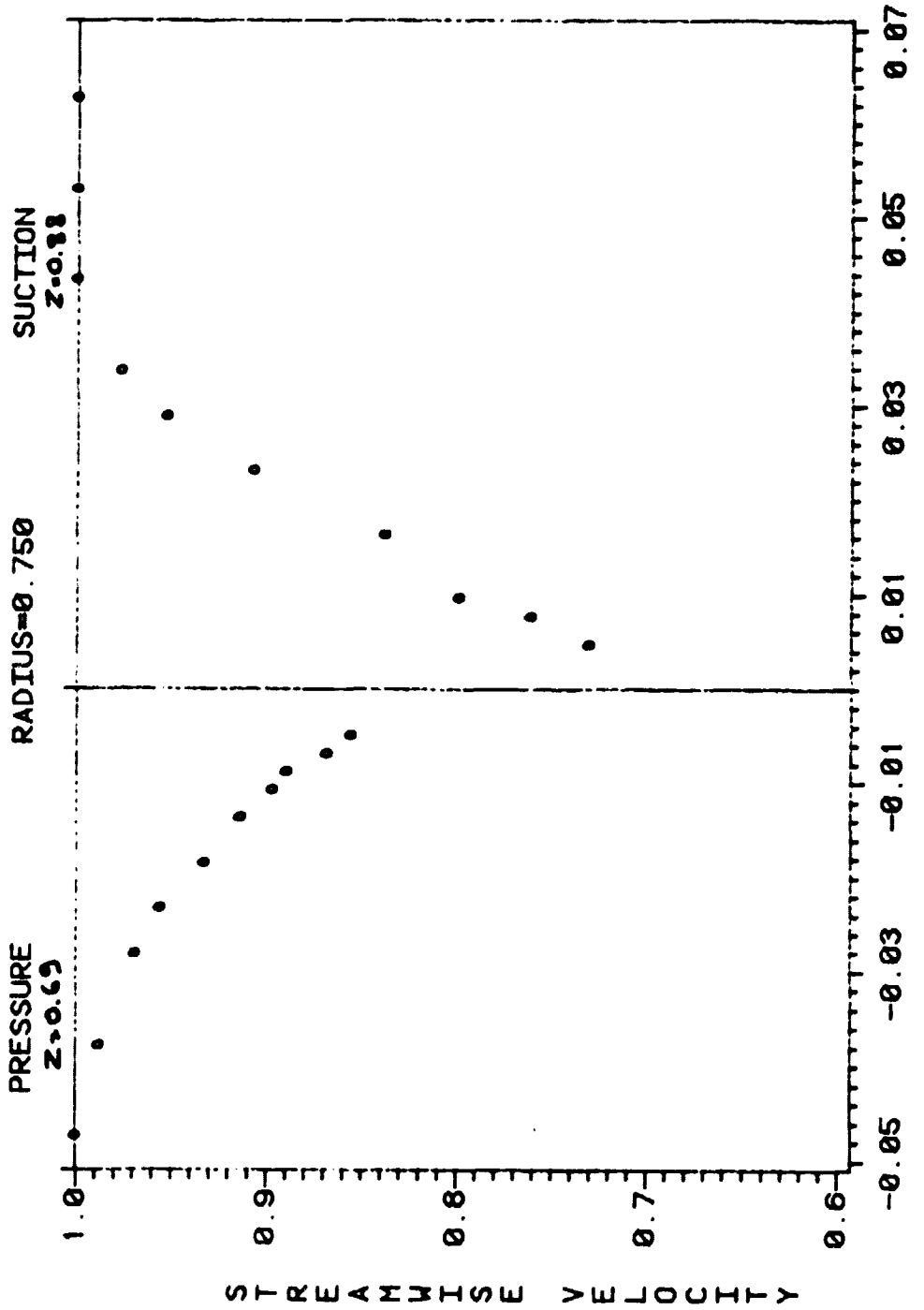

Figure 15. Streamwise velocity (U_s) profiles, R = 0.75, z = 0.69 (P.S.), z = 0.88 (S.S.)

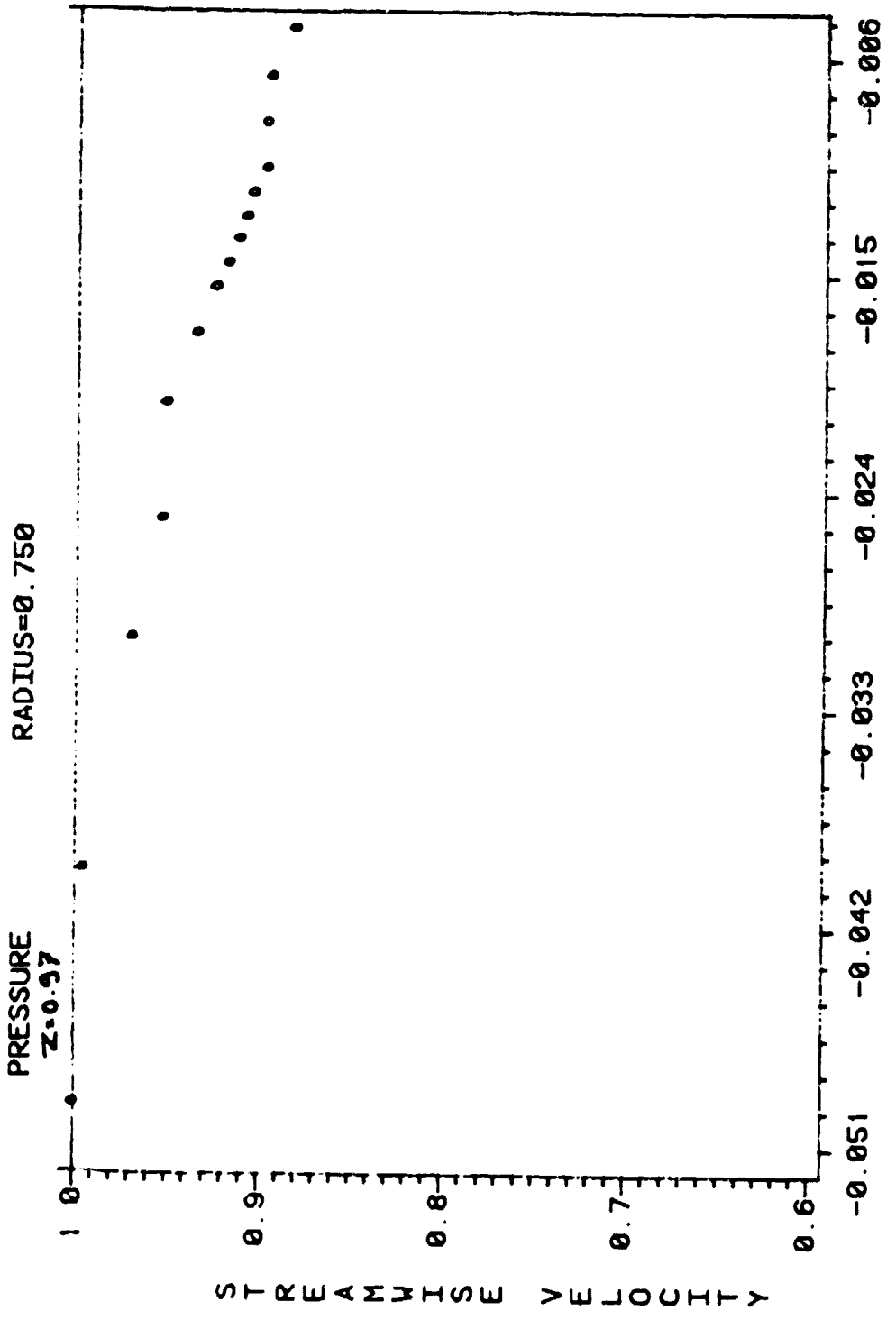

Figure 16. Streamwise velocity (U_s) profile, R = 0.75, z = 0.97 (P.S.)

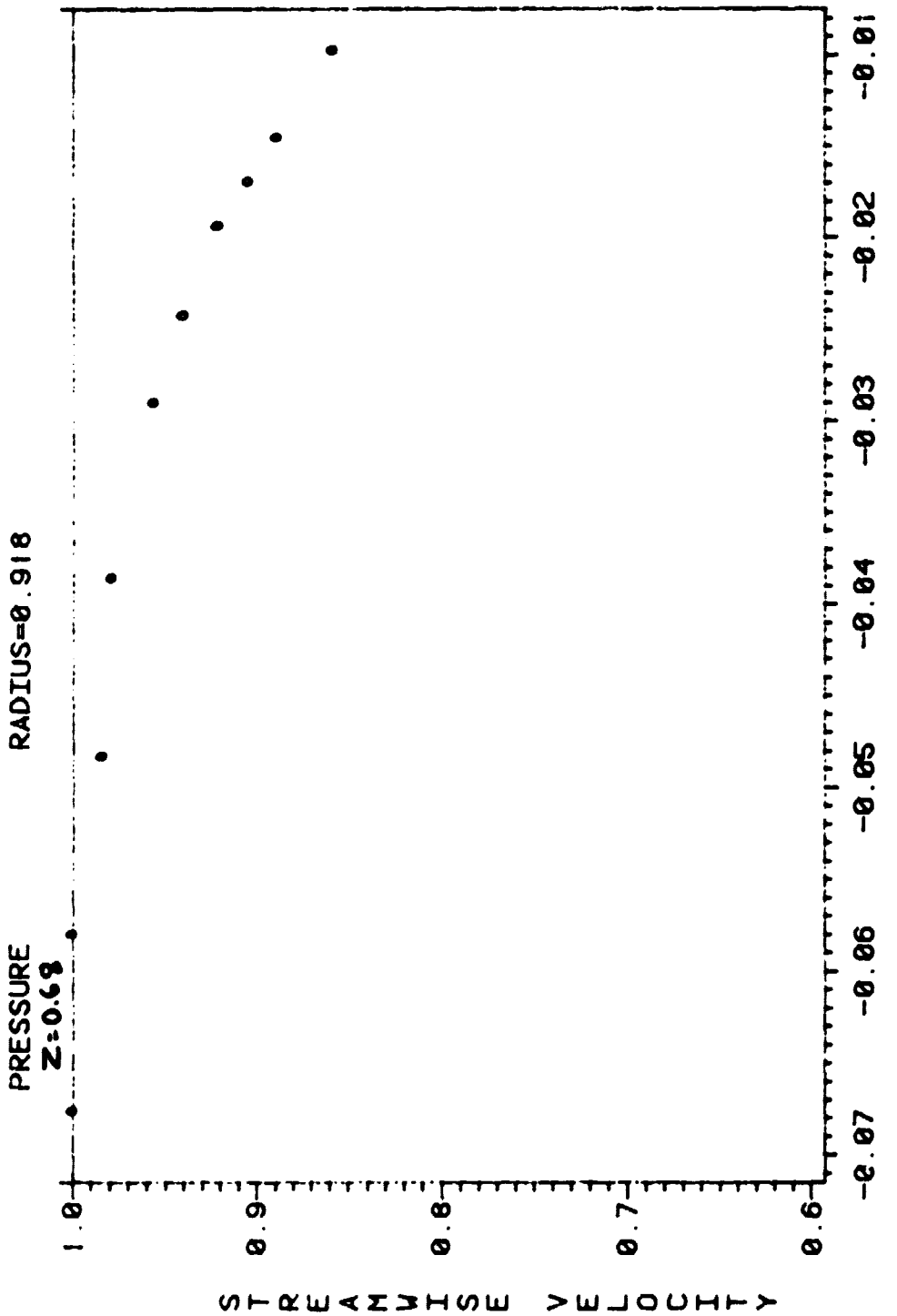

Figure 17. Streamwise velocity (U_s) profile, R = 0.918, z = 0.68 (P.S.)

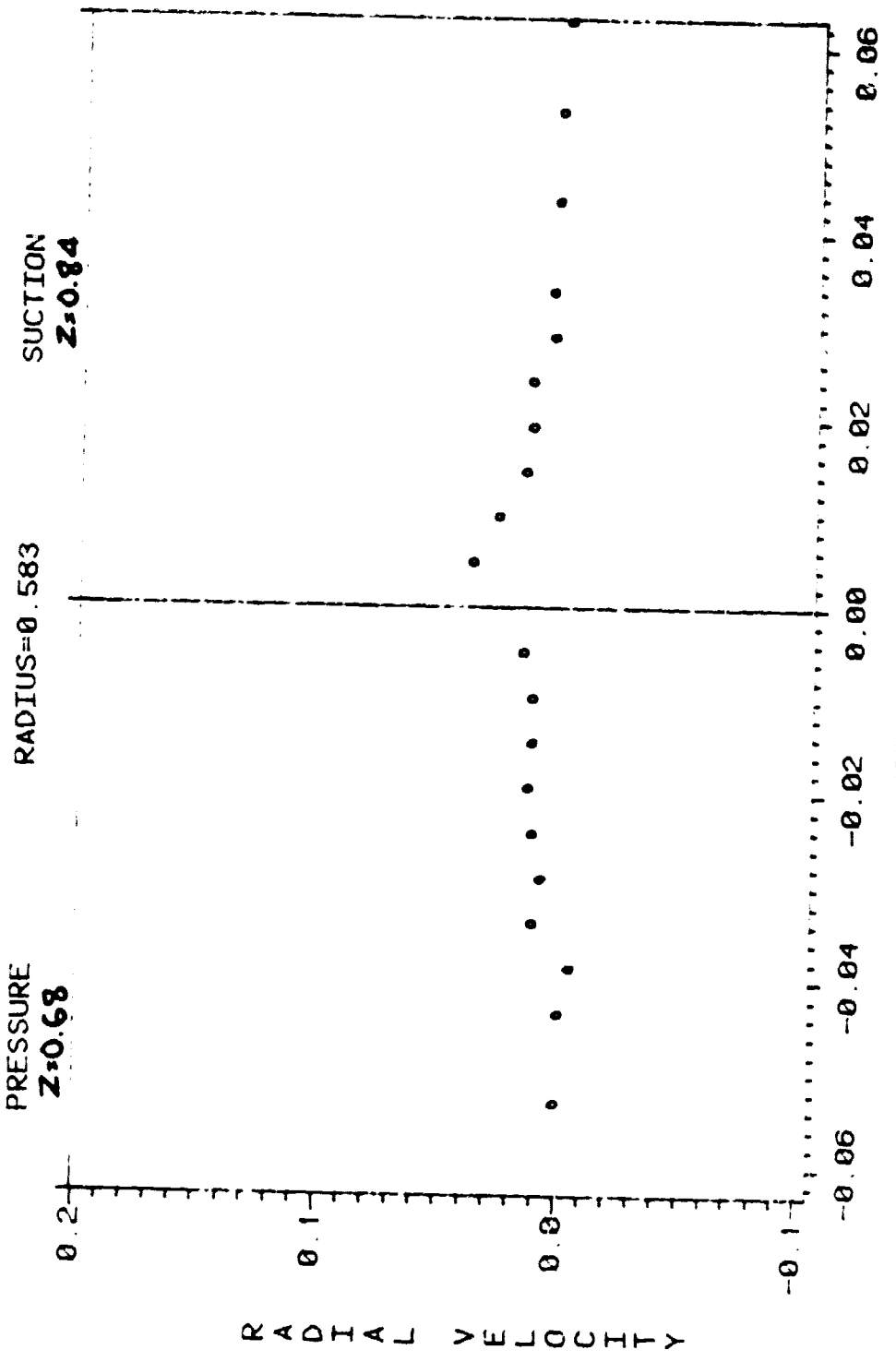

Figure 18. Radial velocity (W) profiles, R = 0.583, z = 0.68 (P.S.), z = 0.84 (S.S.)

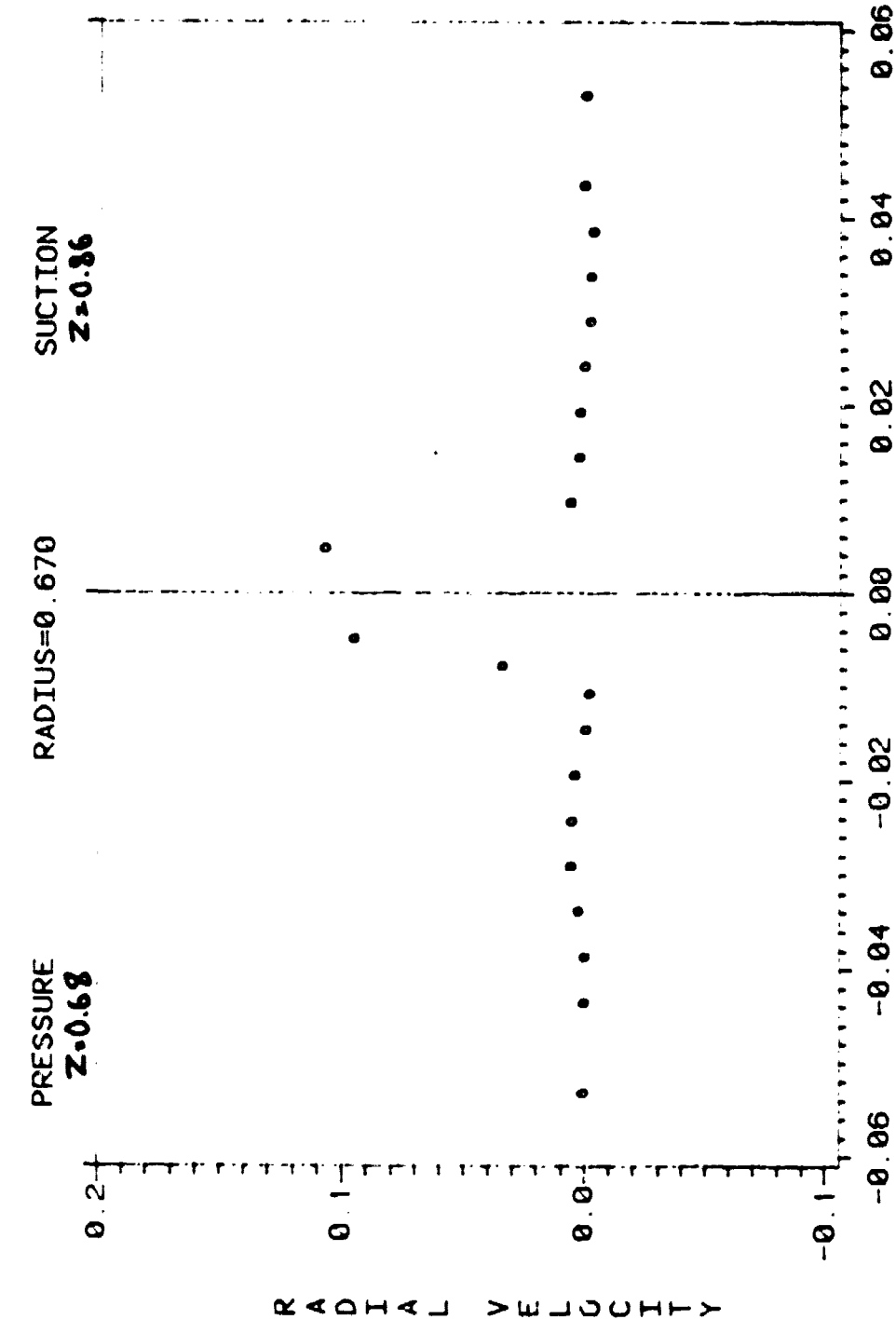

Figure 19. Radial velocity (W) profiles, R = 0.67, z = 0.68 (P.S.), z = 0.86 (S.S.)

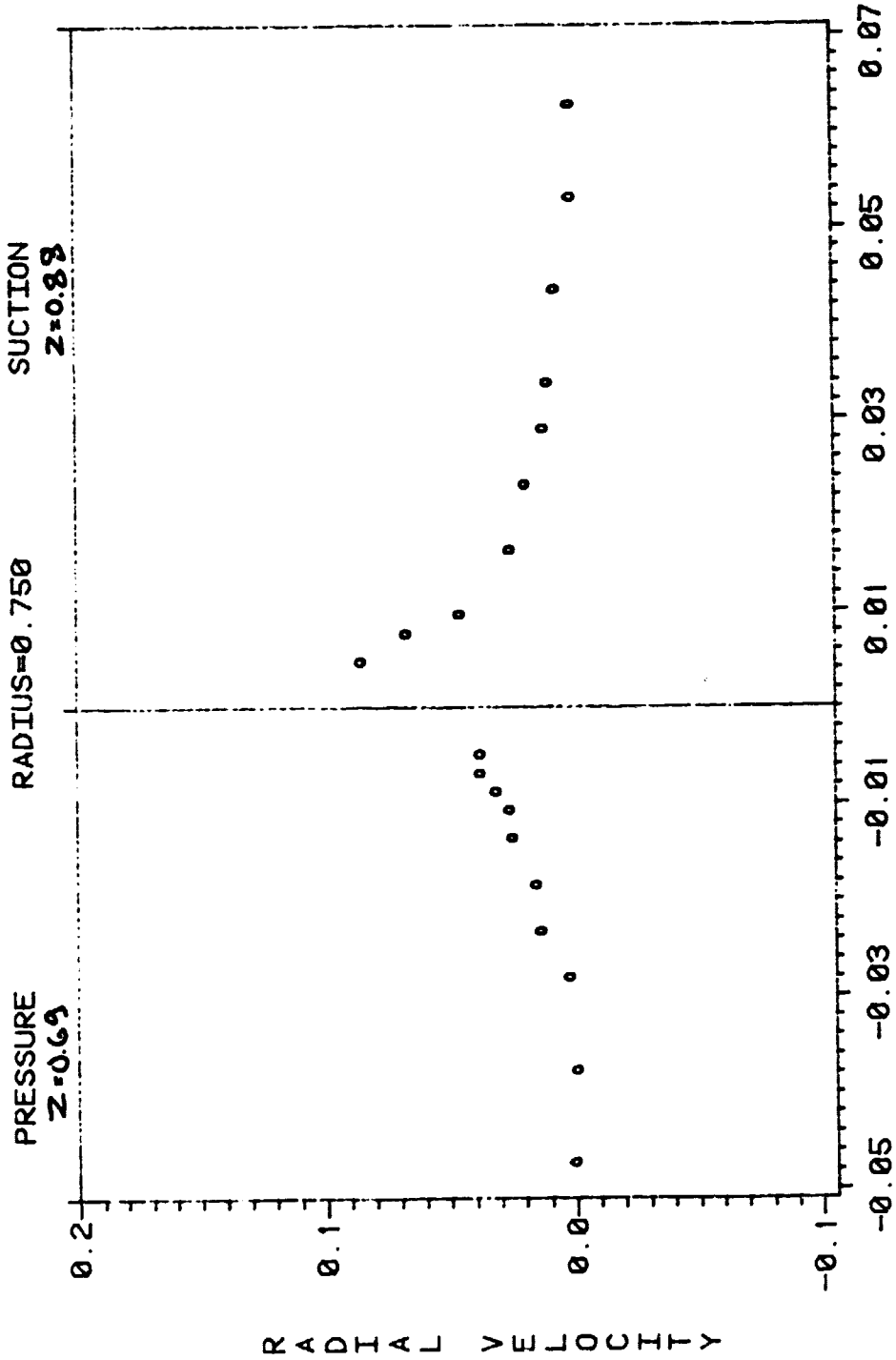

Figure 20. Radial velocity (W) profiles, R = 0.75, z = 0.69 (P.S., z = 0.88 (S.S.)

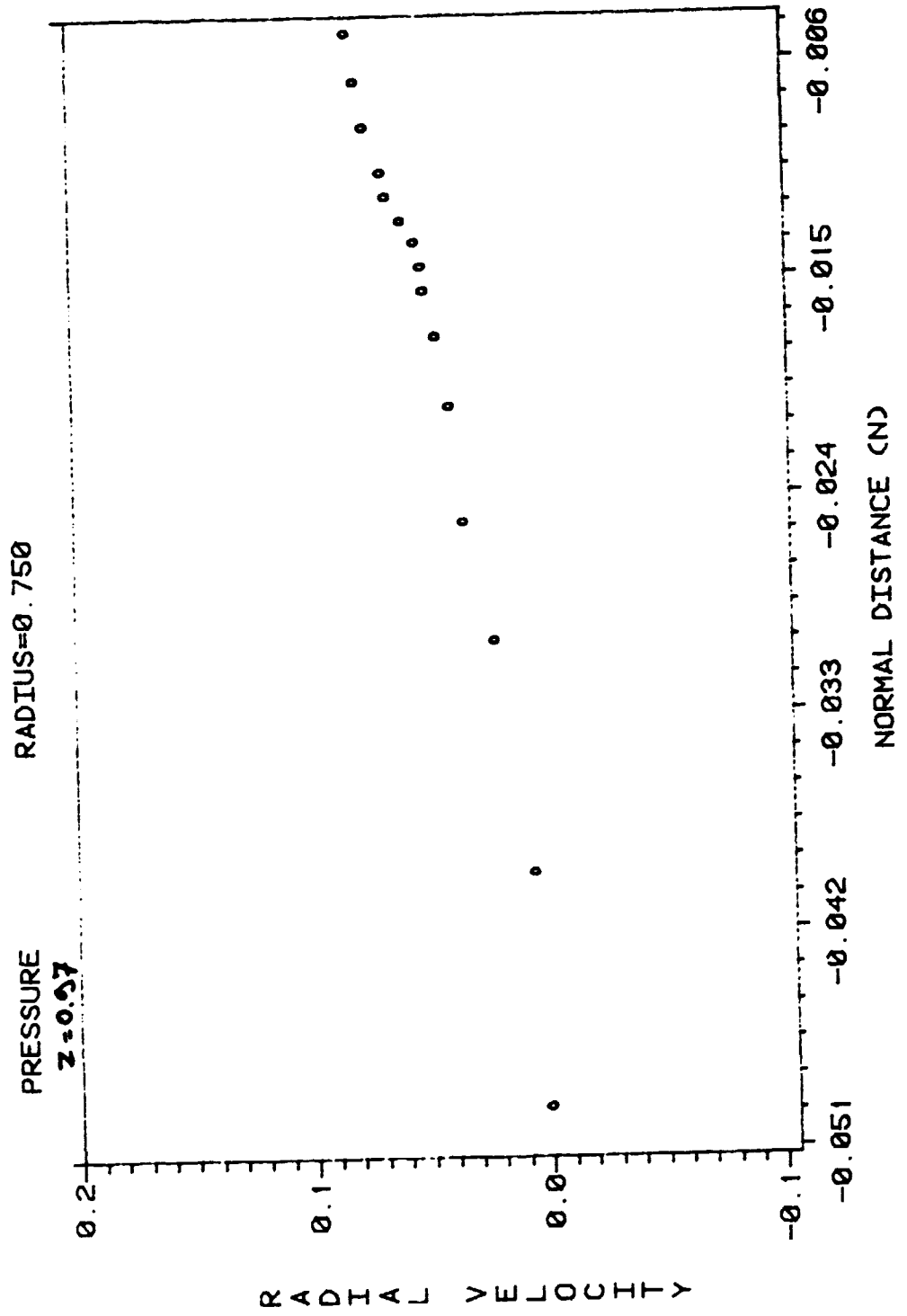

Figure 21. Radial velocity (W) profiles, R = 0.75, z = 0.97 (P.S.)

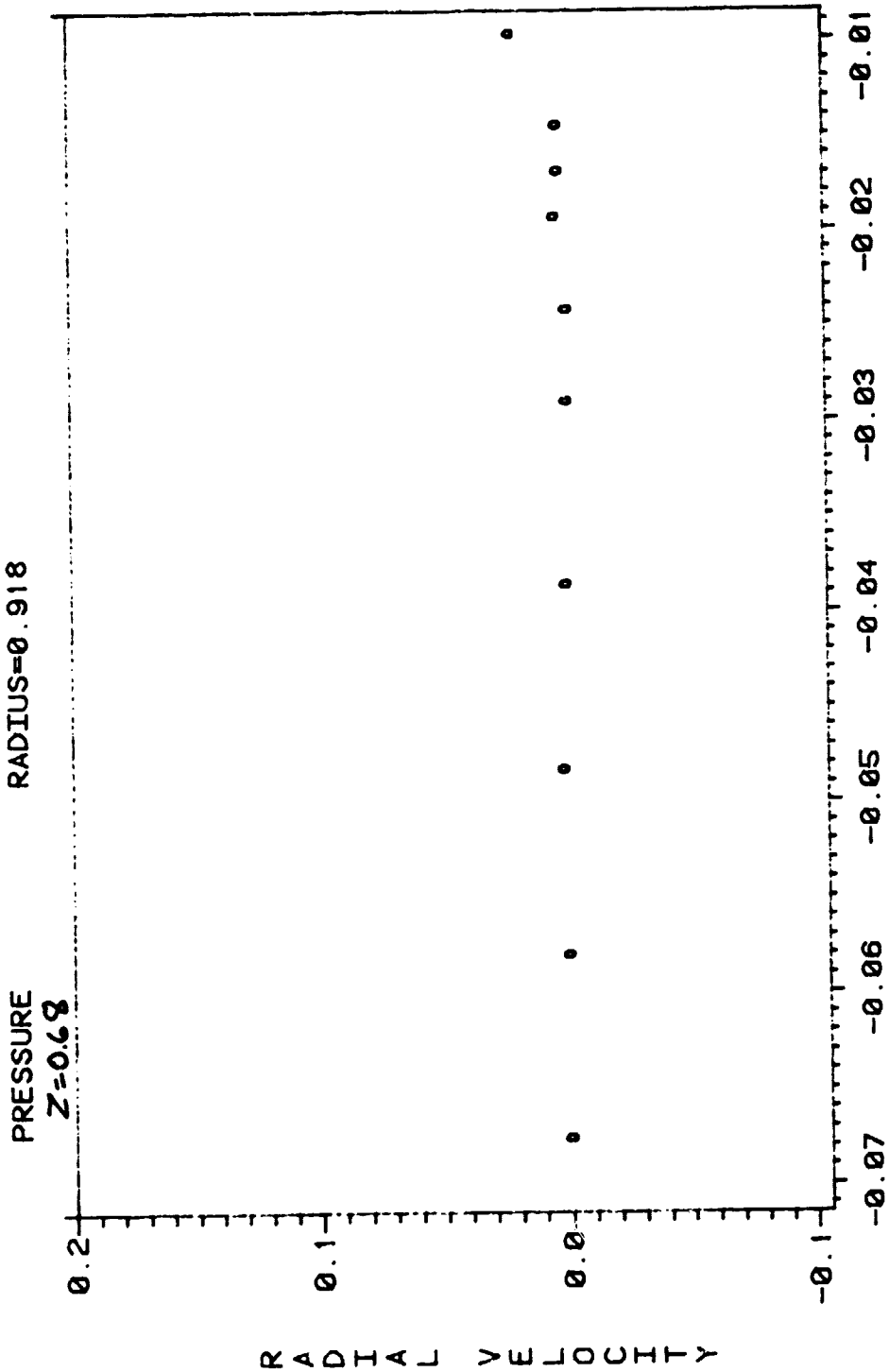

Figure 22. Radial velocity (W) profile, R = 0.918, z = 0.68 (P.S.)

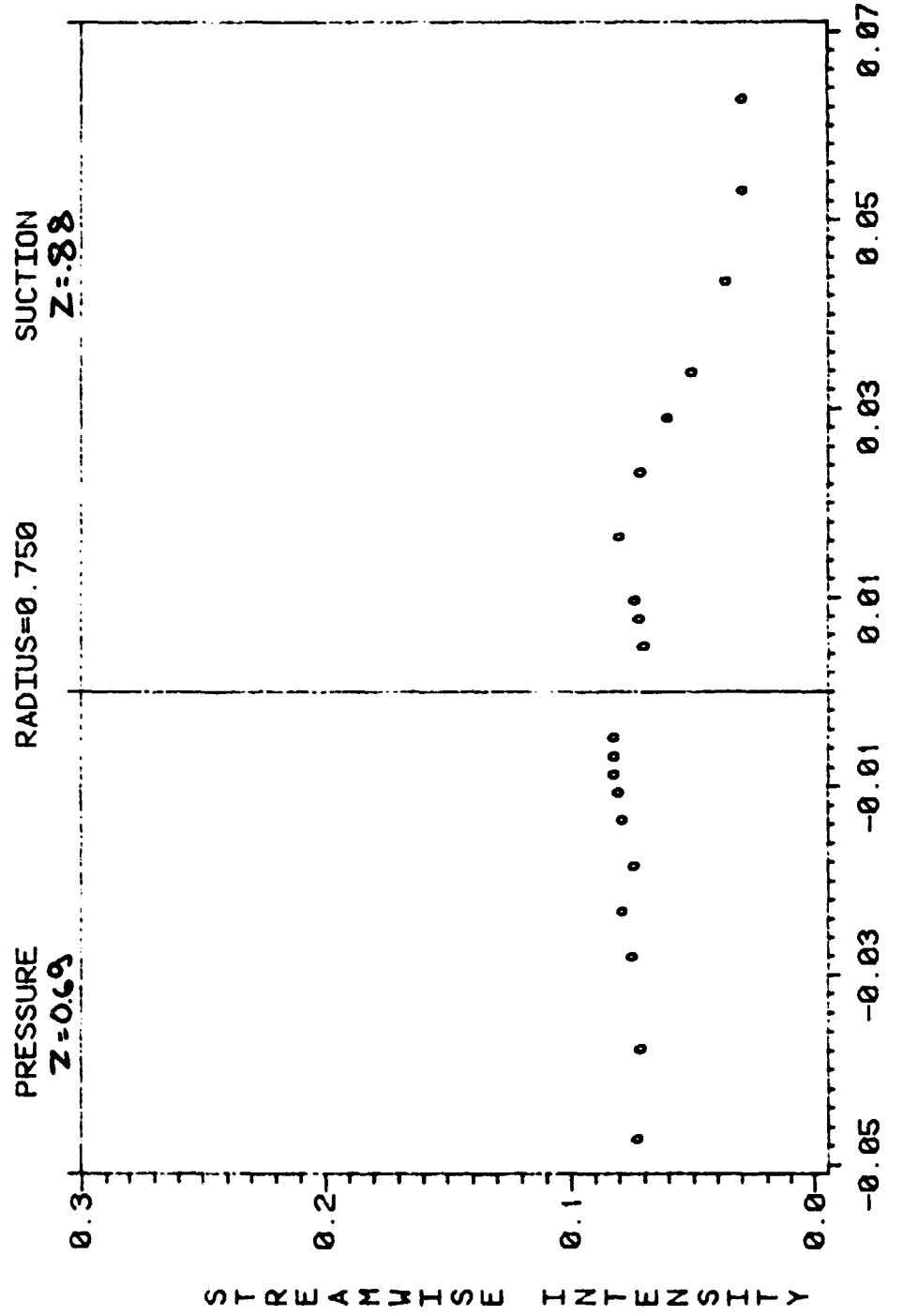

Figure 23. Streamwise turbulent intensity (τ_z) profiles, R = 0.75, z = 0.69 (P.S.), z = 0.88 (S.S.)

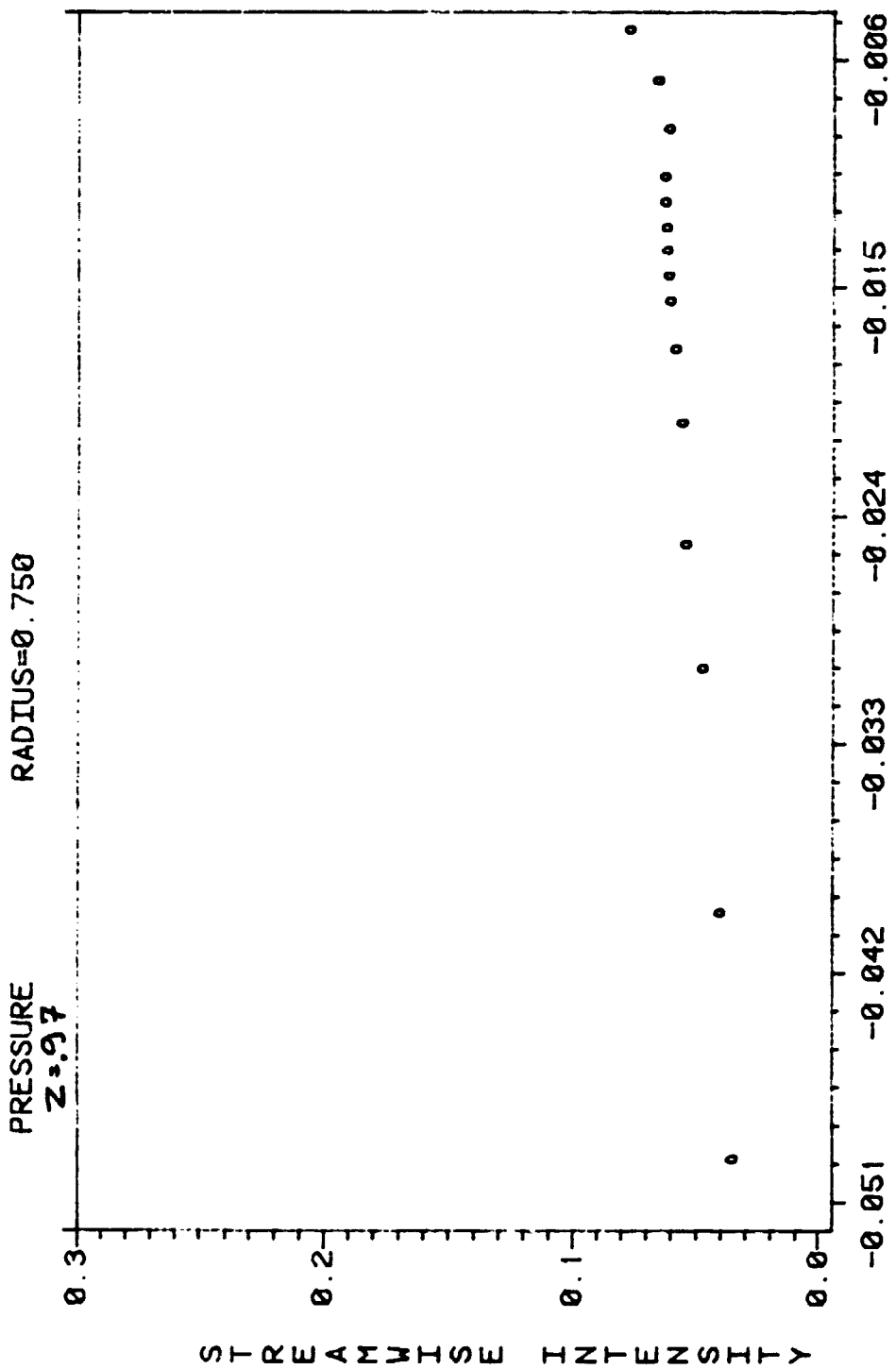

Figure 24. Streamwise turbulent intensity (τ_z) profiles, R = 0.75, z = 0.97 (P.S.)

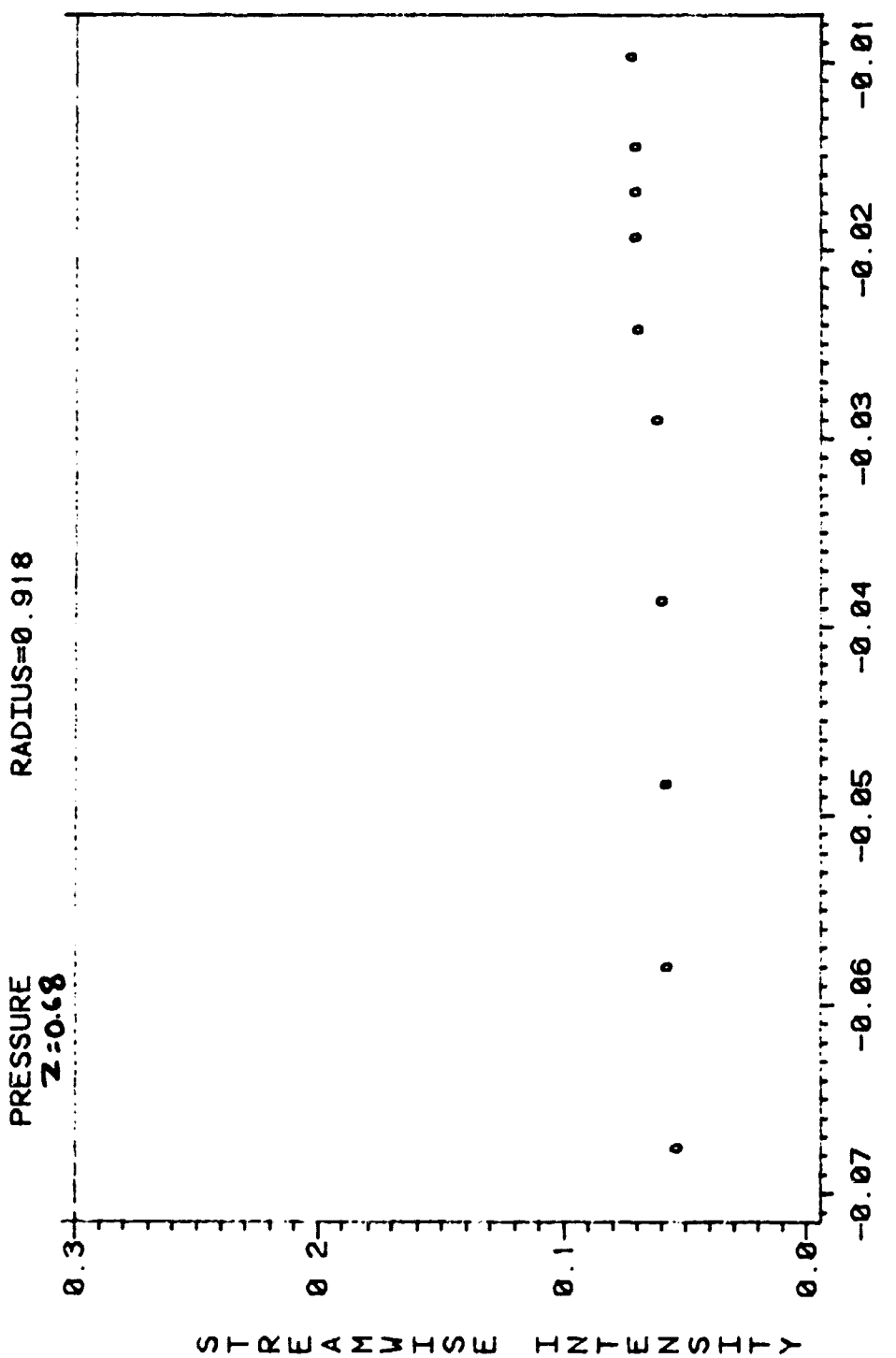

Figure 25. Streamwise turbulent intensity (τ_z) profile, R = 0.918, z = 0.68 (P.S.)

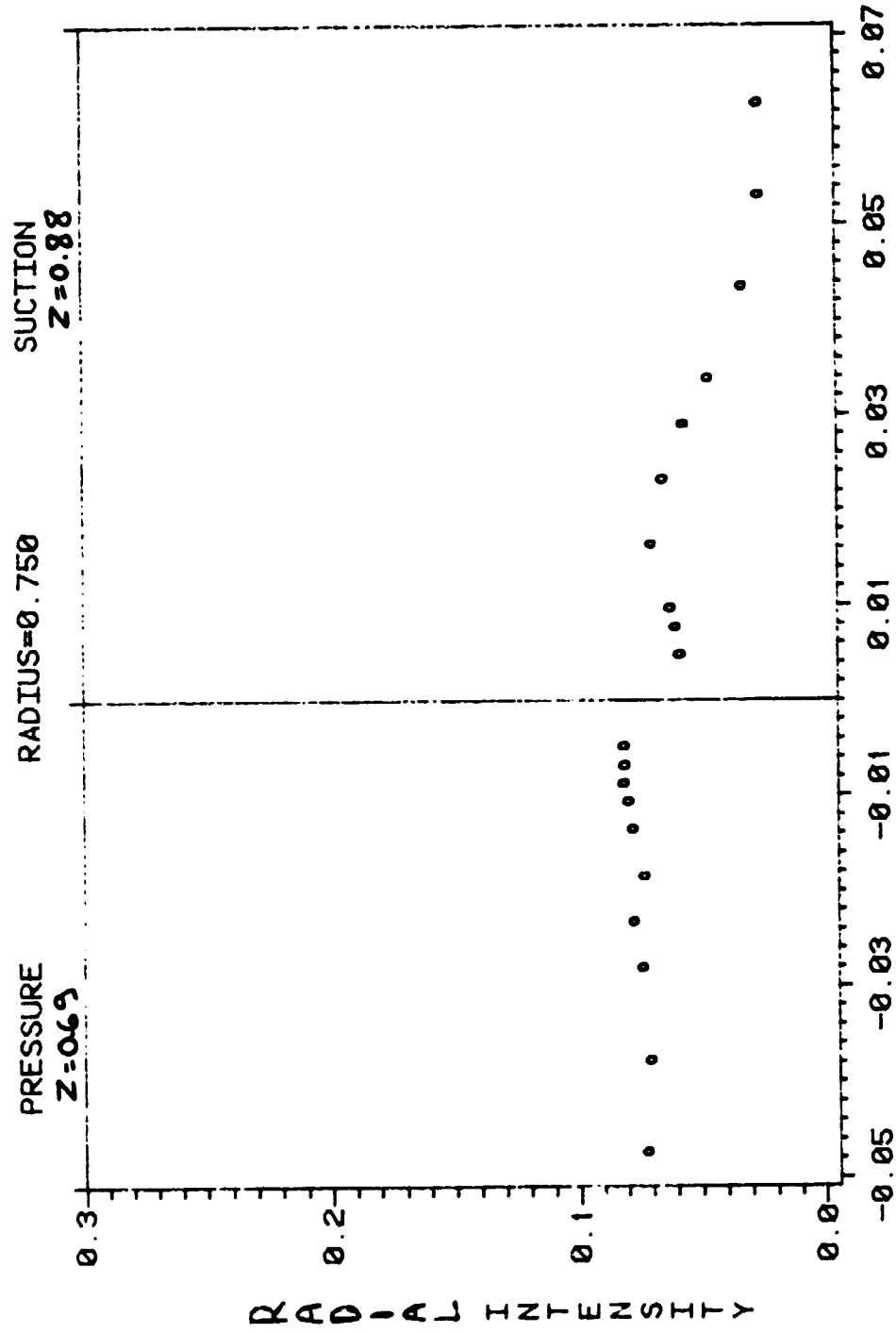

Figure 26. Radial turbulent intensity profiles (τ_r), R = 0.75, z = 0.69 (P.S.), z = 0.88 (S.S.)

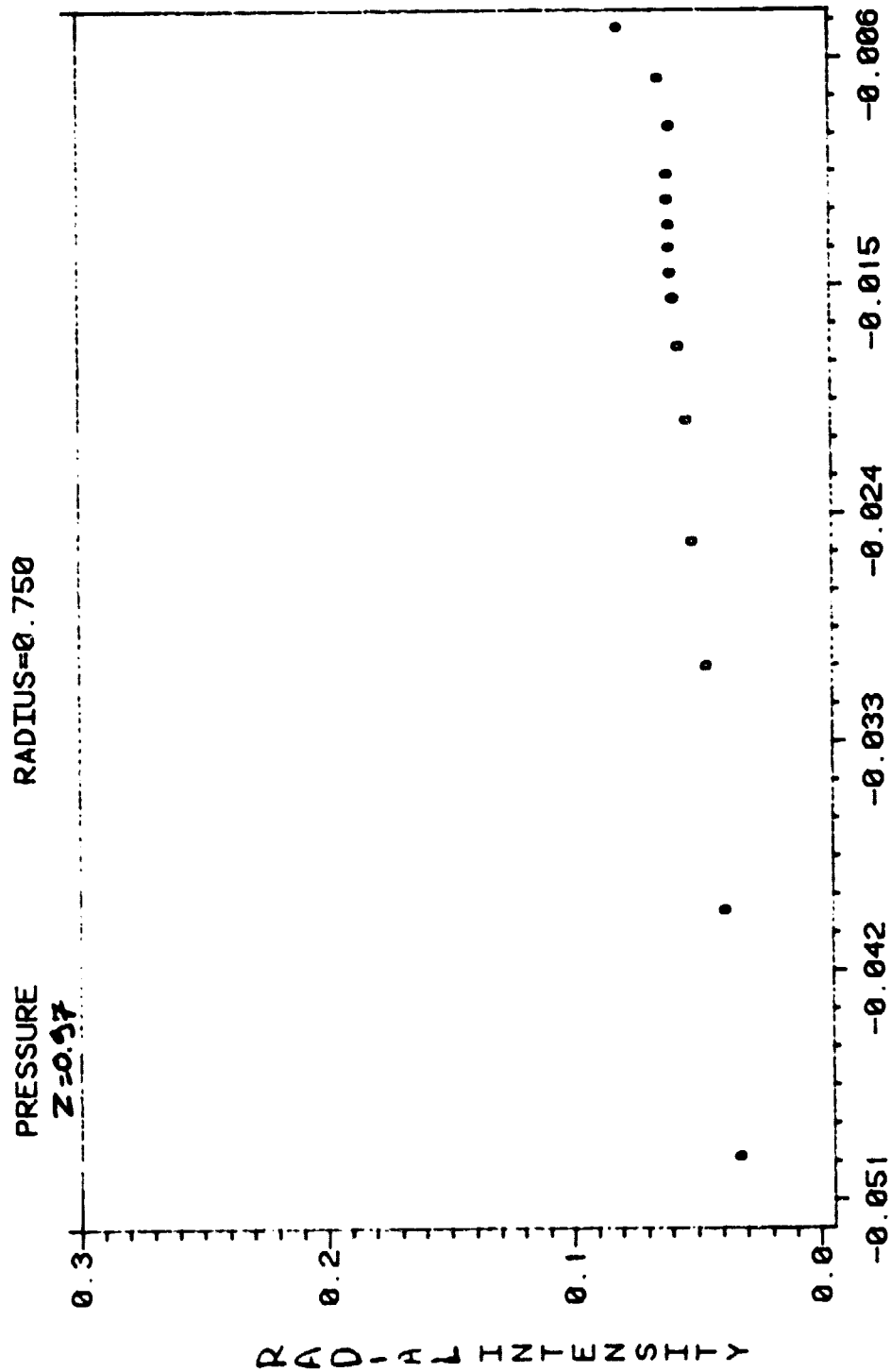

Figure 27. Radial turbulent intensity profile (τ_r), R = 0.75, z = 0.97 (P.S.)

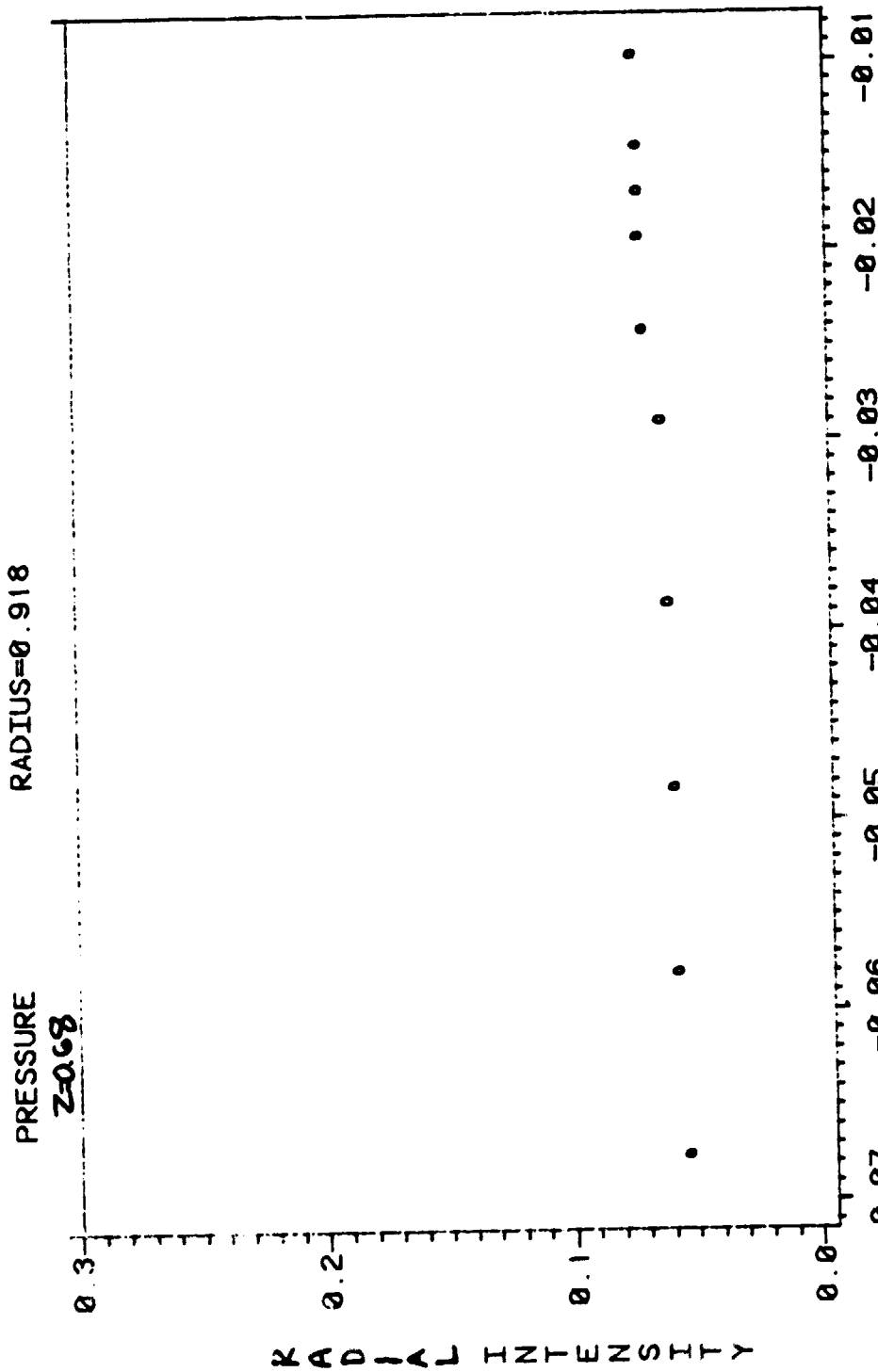

Figure 28. Radial turbulent intensity profiles (τ_r), R = 0.918, z = 0.68 (P.S.)